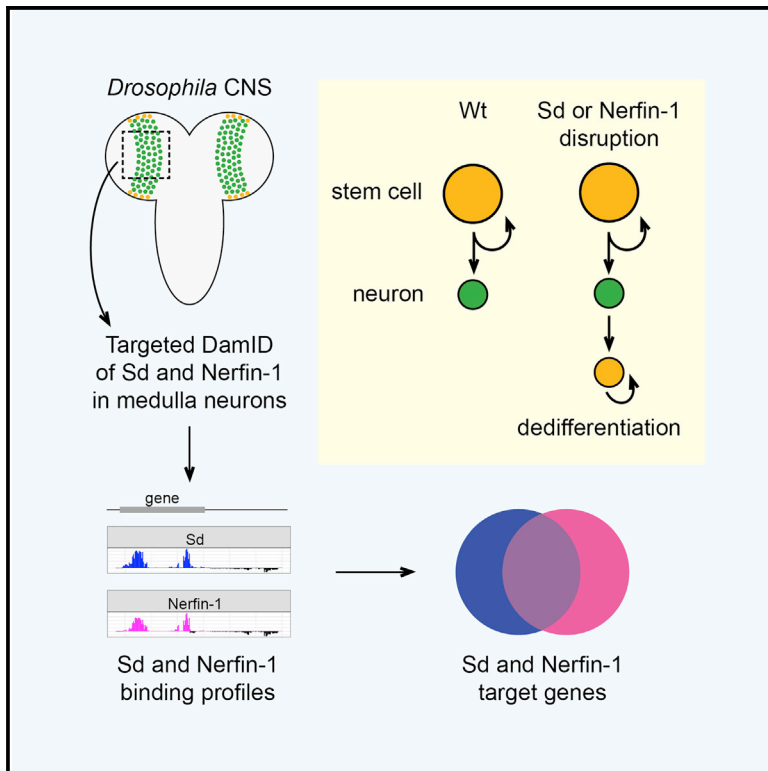


The Scalloped and Nerfin-1 Transcription Factors Cooperate to Maintain Neuronal Cell Fate

Graphical Abstract



Authors

Joseph H.A. Vissers, Francesca Froidi, Jan Schröder, Anthony T. Papenfuss, Louise Y. Cheng, Kieran F. Harvey

Correspondence

kieran.harvey@petermac.org

In Brief

Vissers et al. report that the Scalloped and Nerfin-1 transcription factors physically and functionally interact to maintain medulla neuron fate in the *Drosophila* CNS. Identification of their genome-binding profiles reveal that these transcription factors regulate neuron fate, at least in part, by modulating Notch signaling.

Highlights

- Scalloped and Nerfin-1 form a physical complex in flies and human cells
- Scalloped and Nerfin-1 are essential for maintaining the fate of medulla neurons
- Scalloped and Nerfin-1 occupy a highly overlapping set of genomic loci
- Scalloped and Nerfin-1 regulate neuron fate in part by modulating Notch signaling



The Scalloped and Nerfin-1 Transcription Factors Cooperate to Maintain Neuronal Cell Fate

Joseph H.A. Vissers,^{1,2,10} Francesca Froidi,^{1,2,10} Jan Schröder,^{3,9} Anthony T. Papenfuss,^{1,2,3,4,5} Louise Y. Cheng,^{1,2,8,11} and Kieran F. Harvey^{1,2,6,7,11,12,*}

¹Peter MacCallum Cancer Centre, 305 Grattan Street, Melbourne, VIC 3000, Australia

²Sir Peter MacCallum Department of Oncology, University of Melbourne, Parkville, VIC 3010, Australia

³Bioinformatic Division, Walter and Eliza Hall Institute of Medical Research, Parkville, VIC 3053, Australia

⁴Department of Medical Biology, University of Melbourne, Melbourne, VIC 3010, Australia

⁵Department of Mathematics and Statistics, University of Melbourne, Melbourne, VIC 0310, Australia

⁶Department of Anatomy and Developmental Biology, and Biomedicine Discovery Institute, Monash University, Clayton, VIC, Australia

⁷Department of Pathology, University of Melbourne, Parkville, VIC 3010, Australia

⁸Department of Anatomy and Neuroscience, University of Melbourne, Parkville, VIC 3010, Australia

⁹School of Computing and Information Systems, University of Melbourne, Parkville, VIC 3010, Australia

¹⁰These authors contributed equally

¹¹These authors contributed equally

¹²Lead Contact

*Correspondence: kieran.harvey@petermac.org

<https://doi.org/10.1016/j.celrep.2018.10.038>

SUMMARY

The ability of cells to stably maintain their fate is governed by specific transcription regulators. Here, we show that the Scalloped (Sd) and Nervous fingers-1 (Nerfin-1) transcription factors physically and functionally interact to maintain medulla neuron fate in the *Drosophila melanogaster* CNS. Using Targeted DamID, we find that Sd and Nerfin-1 occupy a highly overlapping set of target genes, including regulators of neural stem cell and neuron fate, and signaling pathways that regulate CNS development such as Notch and Hippo. Modulation of either Sd or Nerfin-1 activity causes medulla neurons to dedifferentiate to a stem cell-like state, and this is mediated at least in part by Notch pathway deregulation. Intriguingly, orthologs of Sd and Nerfin-1 have also been implicated in control of neuronal cell fate decisions in both worms and mammals. Our data indicate that this transcription factor pair exhibits remarkable biochemical and functional conservation across metazoans.

INTRODUCTION

The process of cellular differentiation was once thought to be strictly unidirectional from multipotent progenitor to terminally differentiated cell. However, pioneering studies found that somatic cells can be reprogrammed by nuclear transfer (Gurdon, 1962) and pluripotent stem cells can be induced from fibroblasts (Takahashi et al., 2007), indicating that differentiation is a plastic process. A reversal of differentiation, or dedifferentiation, occurs in many cancers whereby cells lose their identity and proliferate aberrantly (Friedmann-Morvinski and Verma, 2014). One such

cancer is glioblastoma multiforme, the most common human brain malignancy. In a mouse model of this disease, cancerous cells arise from dedifferentiated neurons and astrocytes (Friedmann-Morvinski et al., 2012). Therefore, a molecular understanding of cell fate maintenance should provide insights into the pathogenesis of cancers and inform future utilization of stem cells in the context of regenerative medicine (Firas et al., 2015).

Drosophila melanogaster have facilitated the discovery of key features of neurogenesis, common to both invertebrate and vertebrate CNS development (Homem et al., 2015). The majority of neural stem cells in the *D. melanogaster* CNS (type I neuroblasts) divide asymmetrically to replenish the stem cell pool and also give rise to a daughter cell called the ganglion mother cell (GMC), which divides symmetrically to generate two neurons or glia (Homem and Knoblich, 2012). At each cell division, cell fate determinants are segregated into the GMC to promote its differentiation; and disruption of differentiation can lead to tumorigenesis (Bowman et al., 2008; Wang et al., 2006; Lee et al., 2006; Choksi et al., 2006; Betschinger et al., 2006). However, how the differentiated state of post-mitotic neurons is maintained is less well understood, and here we address this question in the medulla neurons of the *Drosophila* optic lobes.

Dedifferentiation is associated with alterations in chromatin architecture and gene expression, indicating that regulators of transcription are actively required to maintain the differentiated state. In the context of neuronal differentiation, very few transcription factors have been identified that are essential for maintaining neuronal cell fate in the *D. melanogaster* CNS. Two such factors are the zinc finger transcription factor, Nerfin-1 and the BTB-zinc finger transcription factor, Lola. Loss of either protein in CNS neurons causes a striking dedifferentiation phenotype, whereby terminally differentiated neurons revert back to a neuroblast-like fate (Froidi et al., 2015; Southall et al., 2014; Xu et al., 2017). Our previous studies implied that Nerfin-1 maintains neuronal fate by promoting neuronal gene expression and repressing proliferation and stemness genes (Froidi et al., 2015).



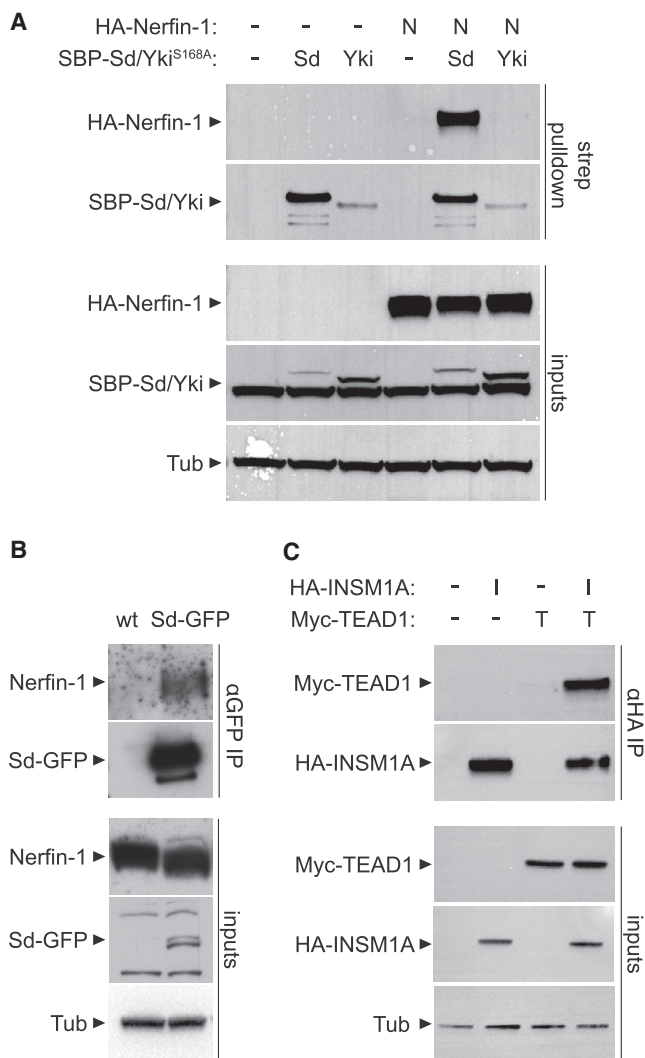


Figure 1. Scalloped and Nerfin-1 Form a Physical Complex Both *In Vitro* and *In Vivo* in *Drosophila*, and This Property Is Conserved in Their Human Orthologs

(A) *D. melanogaster* S2 cells were transfected with the indicated plasmids. Yki and Sd were purified by streptavidin pull-down, and the presence of Nerfin-1 was detected by western blot. Nerfin-1 bound to Sd, but not Yki.

(B) Sd-GFP was immunoprecipitated from brains of stage L3 larvae by anti-GFP nanobodies, and the presence of Nerfin-1 was detected by western blot. Sd-GFP bound to Nerfin-1.

(C) Human 293T cells were transfected with the indicated plasmids. INSM1A was immunoprecipitated by anti-HA antibodies and the presence of TEAD1 detected by western blot. INSM1A bound to TEAD1.

Input lysates are shown below the pull-down blots, together with Tubulin blots, which serve as loading controls.

Transcription factors often act in a combinatorial fashion (Reiter et al., 2017; Spitz and Furlong, 2012), but it is currently unclear whether Nerfin-1 cooperates with other transcription factors to maintain the fate of CNS neurons.

Here, we identify the key Hippo pathway member Sd as a transcription factor that partners Nerfin-1 to maintain the fate of medulla neurons in the optic lobes of the *D. melanogaster* CNS. Sd

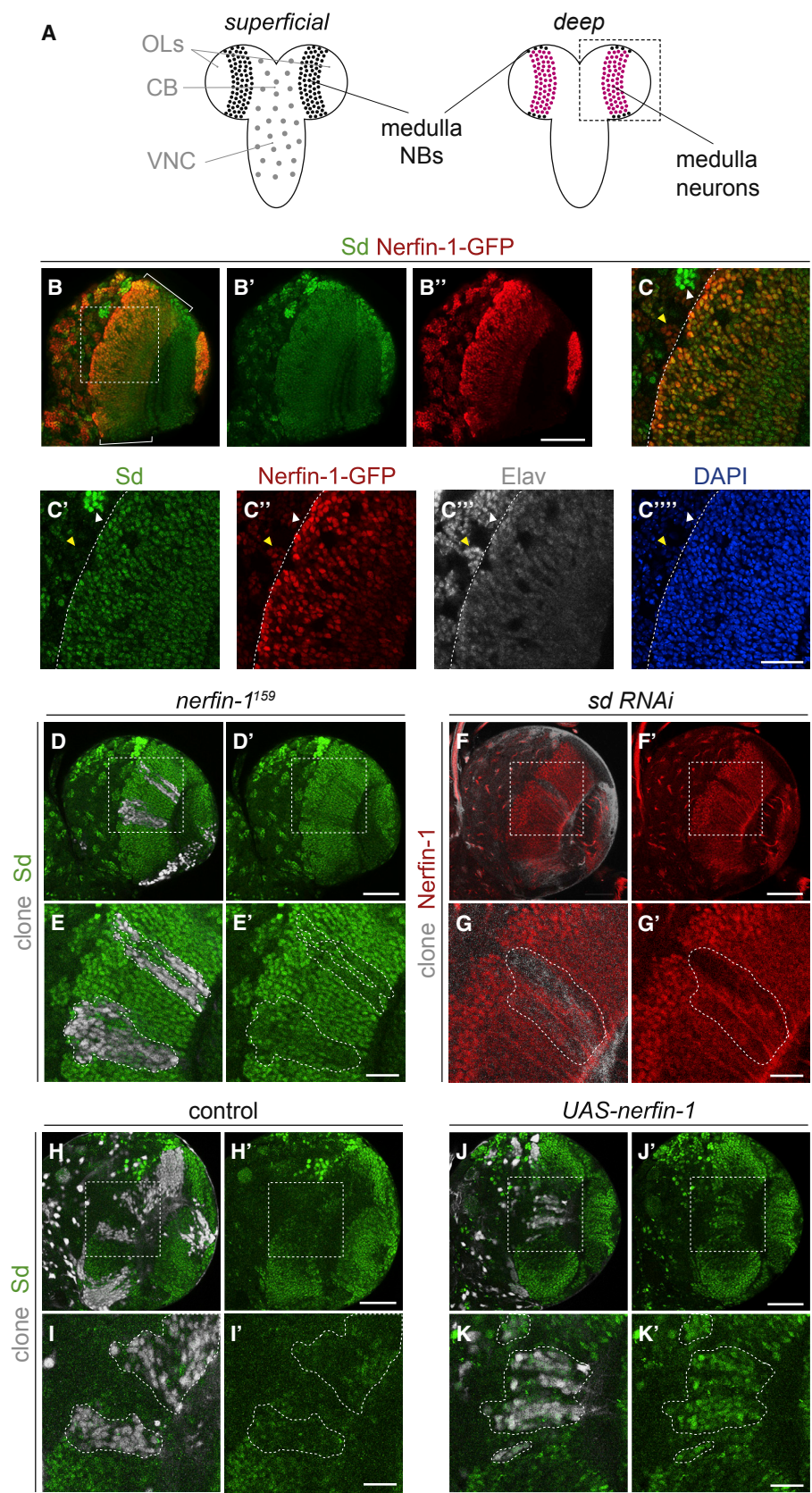
and Nerfin-1 form a physical complex, and both proteins are highly expressed in the medulla neurons of the larval CNS optic lobes. Strikingly, perturbation of either Sd or Nerfin-1 caused medulla neurons to dedifferentiate back to a stem cell-like fate. Using Targeted DamID, we found that these transcription factors occupy a largely overlapping set of target genes including essential mediators of neuroblast and neuron fate, as well as key developmental signaling pathways. Sd and Nerfin-1 maintain neuronal cell fate, at least in part, by regulating expression of Notch pathway genes and activity of this pathway. The human orthologs of Sd and Nerfin-1 (TEAD1 and INSM1) also form a physical complex, suggesting that these proteins are an evolutionarily conserved transcription factor pair.

RESULTS

Scalloped and Nerfin-1 Form a Physical Complex and This Is Conserved in Human Cells

We recently showed that loss of *nerfin-1* in CNS neurons causes a striking dedifferentiation phenotype, whereby terminally differentiated neurons revert back to a neural stem cell-like fate (Froldi et al., 2015). To investigate which transcriptional regulatory proteins Nerfin-1 functions with to control neuronal cell fate, we pursued the TEA domain protein Sd. Sd is the key transcription factor in the Hippo pathway and partners with the Yorkie (Yki) oncoprotein (YAP and TAZ in humans) to regulate organ size (Wu et al., 2008; Zhang et al., 2008a; Goulev et al., 2008). Sd also operates together with Vestigial to control differentiation of the wing and in sensory organ precursor cells, which constitute part of the peripheral nervous system (PNS) (Halder et al., 1998; Simmonds et al., 1998; Williams et al., 1993). We focused on Sd because (1) it was reported to physically interact with Nerfin-1 in an unbiased protein-protein interaction study (Rhee et al., 2014); (2) the *C. elegans* orthologs of Sd and Nerfin-1, EGL-44 and EGL-46, physically interact and co-ordinately regulate FLP cell fate specification (Wu et al., 2001), as well as promote cell cycle exit of Q neuroblasts (Feng et al., 2013); (3) the mammalian orthologs, TEAD1 and INSM1, both control pancreatic neuroendocrine cell identity (Cebola et al., 2015; Jia et al., 2015a); and (4) a TEAD binding motif was enriched in INSM1 target genes, as determined by INSM1 chromatin immunoprecipitation sequencing (ChIP-seq) in murine pancreatic beta cells (Jia et al., 2015a).

Initially, we sought to verify whether Nerfin-1 could form a complex with Sd, as well as Yki, which was also reported to interact with Nerfin-1 (Rhee et al., 2014). *D. melanogaster* S2 cells were transfected with epitope-tagged plasmids expressing the above proteins and Yki and Sd were affinity purified. Nerfin-1 was detected by western blot only in Sd purifications, indicating that it can bind to Sd but not Yki (Figure 1A). To determine whether endogenous Sd and Nerfin-1 form a physical complex, we performed immunoprecipitation experiments on protein lysates prepared from third-instar larval brain lobes dissected from a *D. melanogaster* strain expressing an Sd-GFP fusion protein at endogenous levels and in the endogenous expression pattern (Figures S1A–S1B') (Buszczak et al., 2007; Djiane et al., 2013; Neto-Silva et al., 2010). We used GFP-trap beads to affinity purify Sd and then immunoblotted using a Nerfin-1



(legend on next page)

antibody and revealed that Sd and Nerfin-1 can form a physical complex (Figure 1B). To determine whether the human orthologs of these transcription factors interacted in human cells, we transfected 293T cells with epitope-tagged plasmids expressing TEAD1 and INSM1A and performed immunoprecipitations. A robust interaction was detected, showing that Sd and Nerfin-1, and their human homologs TEAD1 and INSM1A, both form physical complexes (Figure 1C). These findings, coupled with a published report that the *C. elegans* orthologs of these proteins (EGL-44 and EGL-46) physically interact (Feng et al., 2013), raise the possibility that Sd and Nerfin-1 are an evolutionarily conserved transcription factor pair.

Scalloped and Nerfin-1 Are Co-expressed in Medulla Neurons of the CNS Optic Lobes

Next, we assessed Sd and Nerfin-1 expression in the larval *D. melanogaster* CNS. To detect Sd, we used the Sd-GFP strain (Buszczak et al., 2007; Djiane et al., 2013; Neto-Silva et al., 2010) and an Sd antibody (Guss et al., 2013). Nerfin-1 expression was detected using an antibody and a *D. melanogaster* strain expressing Nerfin-1-GFP from its endogenous regulatory regions and which faithfully recapitulates its expression domain (Kuzin et al., 2007). *D. melanogaster* neural progenitor cells produce a number of different cell types in a distinct temporal order, where the deepest layer of neurons forms first, and later-born neurons are located on the outer layers of the CNS (Brand and Livesey, 2011). In the optic lobes, symmetrically dividing neuroepithelial cells differentiate into medulla neuroblasts mostly located on the CNS surface (Figure 2A, black). These neuroblasts divide asymmetrically to generate medulla neurons (Figure 2A, pink), which occupy the deeper layers of the CNS close to the medulla neuropil (Egger et al., 2007; Yasugi et al., 2008). In optic lobe neuroblasts, Nerfin-1 expression could not be detected, while expression of Sd was detectable at low levels (Figures S1C–S1F'). By contrast, Sd was strongly expressed in the *Elav*⁺ medulla neurons and its expression domain closely overlapped with that of Nerfin-1 (Figures 2B–2C''' and S1G–S1H''). To investigate potential regulatory relationships between Sd and Nerfin-1, we genetically modified expression of each protein

and examined any impact on the reciprocal protein. We used the hsFlp-MARCM technique and a null allele of *nerfin-1* (*nerfin-1*¹⁵⁹ [Kuzin et al., 2005]) to generate mutant clones, and found that Sd expression was downregulated (Figures 2D–2E'). Similarly, in actin-Gal4 flip-out clones in medulla neurons where Sd was depleted by RNAi, Nerfin-1 expression was lowered (Figures 2F–2G'). In the converse experiment, overexpression of Nerfin-1 caused elevation of Sd but this was only obvious in older medulla neurons in deep sections of the optic lobe, which normally express lower levels of Sd (Figures 2H–2K'). By contrast, overexpression of Sd did not affect Nerfin-1 expression (Figures S2A–S2B'). Overall, these data show that, as well as being able to form a physical complex, the abundance of Sd and Nerfin-1 in the larval CNS can be influenced by the relative abundance of each protein.

Perturbation of Scalloped and Nerfin-1 Induces Dedifferentiation of Medulla Neurons

Previously, we showed that Nerfin-1 is essential for maintenance of neuronal fate in the neuroblast lineages of the ventral nerve cord and central brain (Froldi et al., 2015). To investigate its role in medulla neurons, we generated *nerfin-1*¹⁵⁹ mutant clones using the MARCM technique. In control clones, deep optical sections (~15 μm deep) consisted only of post-mitotic neurons, characterized by the absence of the neuroblast marker Mira (Figures 3A–3B'). By contrast, several ectopic pH3⁺/Mira⁺ cells were observed in equivalent sections through *nerfin-1*¹⁵⁹ clones in the medulla cortex (Figures 3C–3D', 3I, and S2I–S2I'), indicating that Nerfin-1 is required to maintain neuronal differentiation status in multiple CNS regions. To investigate a role for Sd in the control of medulla neuron fate, we generated actin-Gal4 flip-out clones that expressed an *sd* RNAi transgene. As in *nerfin-1*¹⁵⁹ clones, we observed ectopic pH3⁺/Mira⁺ cells in deep layers of the medulla cortex (Figures 3E–3F', 3I, and S2J–S2J'), a CNS region that is normally occupied by post-mitotic neurons. Next, we further examined a role for Sd in medulla neurons using a transgene that encodes an Sd protein (*Sd-GA*), whereby the yeast Gal4 activation domain has been fused to Sd to override its default repressor function, thus causing it to dominantly

Figure 2. Scalloped and Nerfin-1 Are Co-expressed in Optic Lobe Medulla Neurons and Influence Each Other's Abundance

(A) Schematic representation of the larval CNS, with optic lobes (OLs), ventral nerve cord (VNC), and the central brain (CB) indicated. Medulla neuroblasts (NBs) (black) are observed in superficial CNS sections and medulla neurons (magenta) in deep CNS sections. In all subsequent low-magnification microscopy images, one optic lobe is imaged (boxed region).

(B–C''') Sd (green, detected with an Sd antibody) and GFP-tagged Nerfin-1 (Nerfin-1-GFP, red) are both predominantly expressed in *Elav*⁺ medulla neurons (gray, C'''). Nuclei are stained with DAPI (blue, C'''). The boxed region in (B) is magnified in (C)–(C''') where the boundary between the medulla neurons (right) and the CB neurons (left) is indicated with a dotted line.

In the CB, some clusters of neurons showed high Sd expression and low Nerfin-1-GFP expression (white arrowhead), while others showed the opposite pattern (yellow arrowhead).

(D–E') Sd expression (green, detected with an Sd antibody) was reduced in *nerfin-1*¹⁵⁹ MARCM clones located in the medulla neuron layer of larval brain lobes (grayscale). The boxed areas in (D) and (D') are magnified in (E) and (E'); clones are outlined.

(F–G') Reduced Nerfin-1 expression (red, detected with an antibody) in *sd*-RNAi flip-out clones (gray) located in the medulla neuron layer of a larval optic lobe. The boxed regions in (F) and (F') are magnified in (G) and (G'); clones are outlined.

(H–K') Sd expression (green, detected with an Sd antibody) was increased in UAS-*nerfin-1* flip-out clones (J–K') in comparison to control clones (H–I') in the deeper medulla neuron layer of a larval optic lobe. Clones are marked in grayscale. The boxed regions in (H) and (H') and (J) and (J') are magnified in (I) and (I') and (K) and (K'), respectively, and clones are outlined.

For the experiments shown in (D)–(K'), clones were induced 48 hr after egg laying (AEL) and analyzed 72 hr later and, in the case of (F)–(K'), larvae were shifted to 29°C after clone induction.

Scale bars: 50 μm in (B)–(B''), (D) and (D'), (F) and (F'), (H) and (H'), and (J) and (J'), and 20 μm elsewhere.

See also Figures S1 and S2.

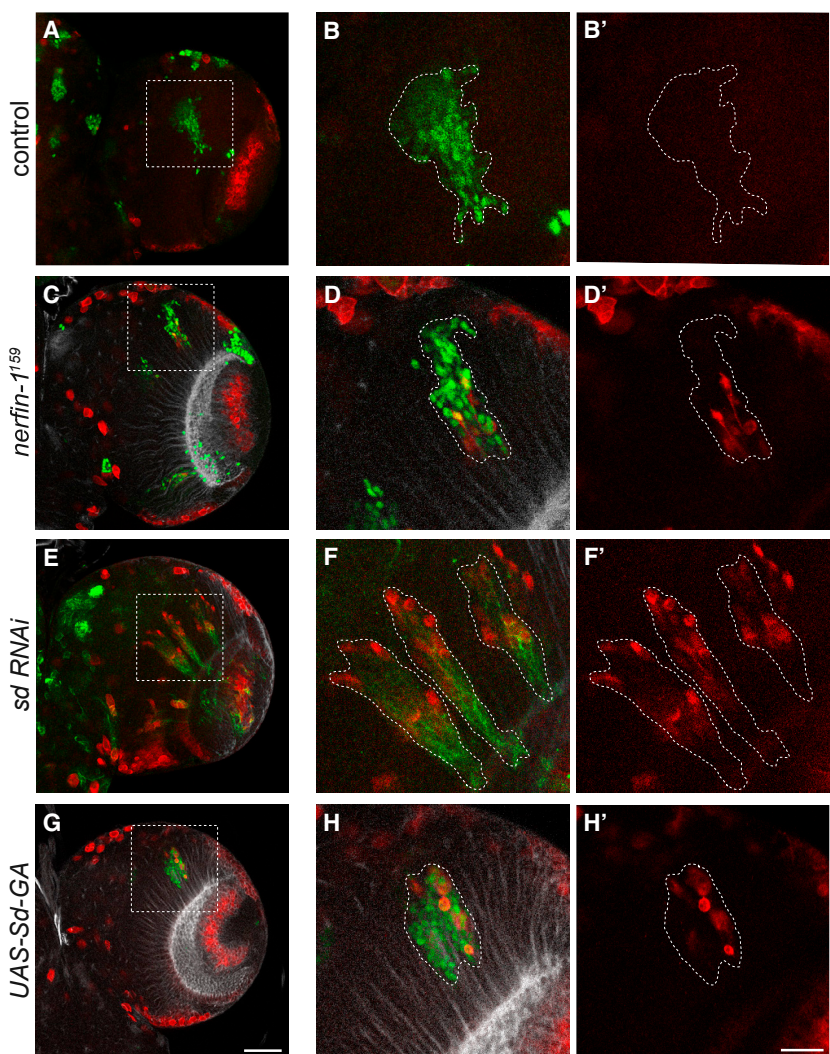


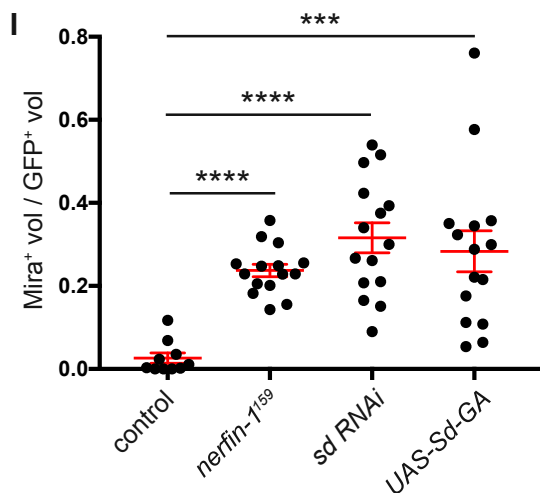
Figure 3. Scalloped and Nerfin-1 Prevent Ectopic Neuroblast Formation in the Medulla

(A–H') Mira (red) and F-actin (phalloidin, grayscale) expression in third-instar larval CNSs containing wild-type control (A–B'), *nerfin-1¹⁵⁹* mutant (C–D'), *sd-RNAi* (E–F'), or *Sd-GA*-expressing (G–H') medulla clones (outlined, green) generated using the MARCM (A–B', C–D', and G–H') or flip-out technique (E–F'). The boxed regions in (A), (C), (E), and (G) are magnified in (B) and (B'), (D) and (D'), (F) and (F'), and (H) and (H'), respectively, and clones are outlined. Ectopic Mira⁺ neuroblasts were found in the medulla neuron layer of the optic lobes in *nerfin-1¹⁵⁹* mutant, *sd RNAi* and *Sd-GA*-expressing, but not control medulla clones. Clones were induced 48 hr AEL and analyzed 72 hr later. In the case of (E)–(F'), larvae were shifted to 29°C after clone induction.

(I) Quantification of Mira⁺ cells (expressed as the ratio between Mira⁺ volume and total GFP⁺ clone volume) in clones of the genotypes displayed in (A)–(H'). n = 10 for the control and n = 15 for all other genotypes. Data are represented as mean ± SEM. p values were obtained performing unpaired t test, and Welch correction was applied in case of unequal variances. ****p < 0.0001 and ***p < 0.001.

Scale bars: 50 μm in (A), (C), (E), and (G), and 20 μm elsewhere.

See also Figure S2.



activate expression of its target genes (Zhang et al., 2008a). Clonal expression of *Sd-GA* induced the formation of ectopic pH3⁺/Mira⁺ cells in the deep layers of the medulla cortex

Control clones and clones where either *Sd* (expression of *sd RNAi* or *Sd-GA*) or *Nerfin-1* (*nerfin-1 RNAi* or *nerfin-1¹⁵⁹*) was perturbed were induced and examined at different time points.

(Figures 3G–3H', 3I, and S2K–S2K'), thus phenocopying both *Sd-RNAi* and *nerfin-1¹⁵⁹* clones. Interestingly, expression of *Sd-GA* did not cause neuronal dedifferentiation in the ventral nerve cord and central brain, suggesting that *Sd*, unlike *Nerfin-1*, has a restricted role in controlling the fate of CNS neurons (data not shown). Finally, to investigate epistatic relationships between *Sd* and *Nerfin-1* in medulla neurons, we employed the MARCM technique to induce *nerfin-1¹⁵⁹* clones that also expressed *Sd*, via a UAS-inducible transgene. Expression of *Sd* modestly reduced the rate of dedifferentiation in *nerfin-1¹⁵⁹* clones (Figures S2C–S2E). By contrast, *Nerfin-1* overexpression did not suppress Mira⁺ cell number in *Sd-GA* clones, although we did observe a trend toward significance (Figures S2F–S2H).

Next, we carried out time course experiments to establish the earliest time point at which ectopic neuroblasts (Dpn⁺) arise when *Sd* or *Nerfin-1* function is perturbed.

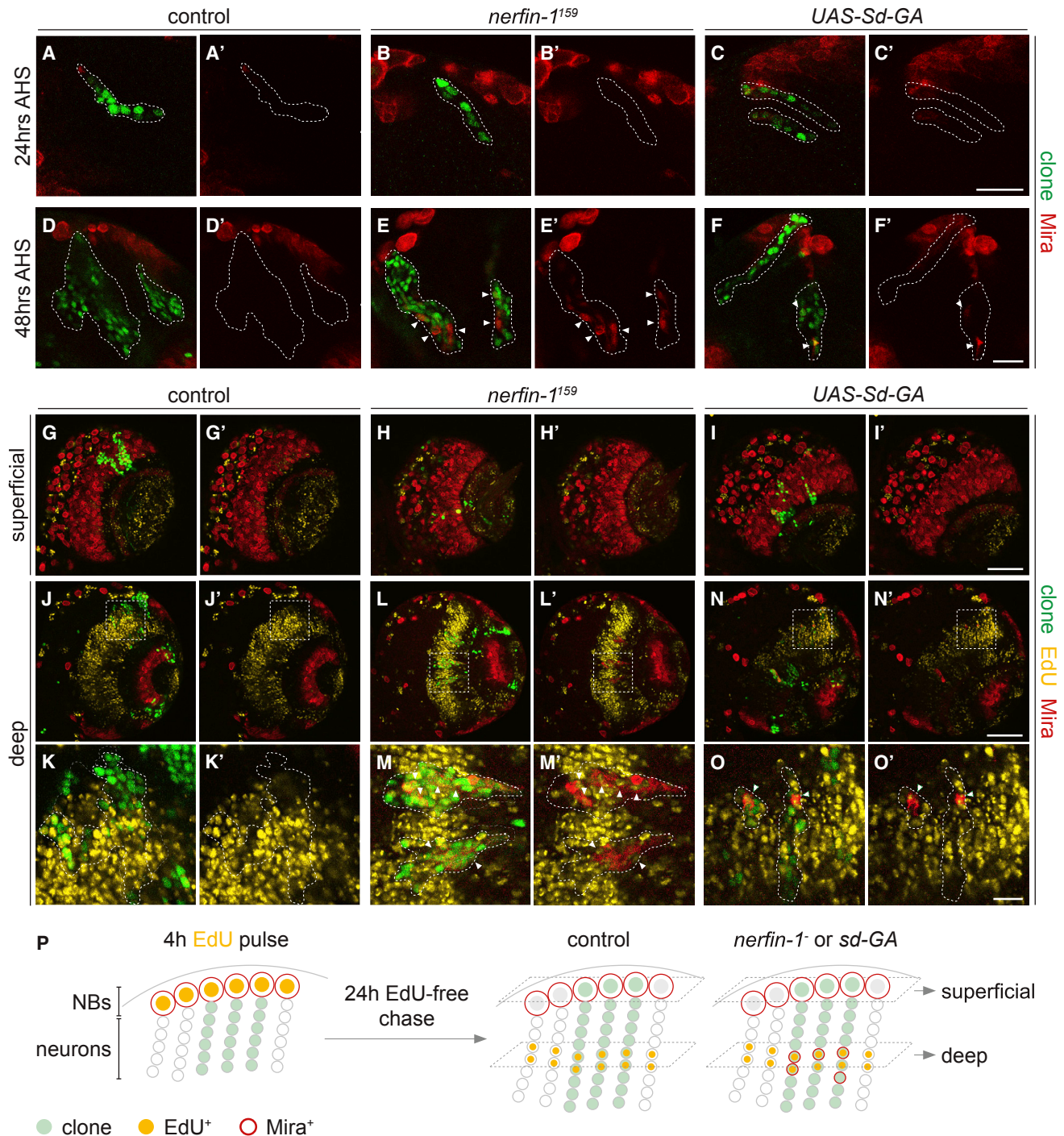


Figure 4. Ectopic Neuroblasts in *nerfin-1* Mutant and *Sd-GA*-Expressing Clones Arise from Dedifferentiation of Medulla Neurons

(A–F) High-magnification images of third-instar larval CNS lobes containing control (A and A' and D and D'), *nerfin-1*¹⁵⁹ mutant (B and B' and E and E'), or *Sd-GA*-expressing (C and C' and F and F') MARCM medulla clones (outlined, and marked by GFP [green]). *nerfin-1*¹⁵⁹ clones and *Sd-GA*-expressing clones contain ectopic Mira⁺ (red) cells (arrowheads) in deep CNS sections at 48 hr but not at 24 hr after heat shock (AHS). Clones in (A)–(C) were induced 96 hr AEL and dissected 24 hr later; clones in (D)–(F) were induced 72 hr AEL and dissected 48 hr later.

(G–O) EdU pulse-chase experiment. Larvae were fed EdU⁺ food for 4 hr 48 hr AHS and then chased with EdU-free food for 24 hr before dissection. Low-magnification images of superficial and deep sections of third-instar larval brain lobes containing control (G and G' and J and J'), *nerfin-1*¹⁵⁹ mutant (H and H' and L and L'), or *Sd-GA*-expressing (I and I' and N and N') medulla MARCM clones (marked by GFP [green]). EdU labeling was absent from the NB-containing superficial sections (G–I'), while it was extensive in the deeper sections where the neuronal progeny resides (J–O'). The clones located in deep sections of the

(legend continued on next page)

16 and 24 hr after clones were induced, clones consisted predominantly of *Elav*⁺ neurons, while only select cells expressed *Dpn* (Figures S3A–S3F'). At these time points, *Mira*, a marker for more mature neuroblasts, was absent from *nerfin-1*¹⁵⁹ and *Sd-GA* clones (Figures 4A–4C'). By 48 hr, control *lacZ RNAi* clones possessed *Elav*⁺ cells (Figures S3G–S3G'), while clones lacking *Nerfin-1* and *Sd* possessed many cells that had dedifferentiated, i.e., they failed to express *Elav* and robustly expressed *Dpn* (Figures S3H–S3I') or *Mira* (Figures 4D–4F', arrowheads). To confirm that ectopic *Mira*⁺ cells in *nerfin-1*¹⁵⁹ and *Sd-GA* clones arise via dedifferentiation, we fed larvae with 5-ethynyl-2'-deoxyuridine (EdU)⁺ food for 4 hr 48 hr after clone induction, and then chased for 24 hr with EdU-free food (Figure 4P). In control animals, EdU was first incorporated by proliferating neuroblasts during the EdU pulse, and inherited by neurons generated during this time window. As new neurons were generated, the proliferating neuroblasts on the surface lost the EdU label (Figures 4G–4I' and 4P), while EdU⁺ neurons were displaced into locations deep within the CNS (Figures 4J–O' and 4P). In *nerfin-1*¹⁵⁹ and *Sd-GA* clones, however, we identified *Mira*⁺ cells that were also EdU⁺ in deep CNS sections normally occupied only by post-mitotic neurons (Figures 4L–4M', 4N–4O', and 4P). This suggests that the cells of origin of these ectopic stem-like cells are differentiated neurons, as opposed to defective progenitor cells, and indicates that *Sd* and *Nerfin-1* play an essential role in the maintenance of medulla neuron fate (Figure 4P). This conclusion is consistent with a recent study on *nerfin-1* function in medulla neurons (Xu et al., 2017) and our finding that *Nerfin-1* is expressed in neurons but not neuroblasts (Figures S1E–S1F').

Sd's best-described function is in the context of Hippo pathway-dependent epithelial tissue growth, where it partners with the *Yki* transcription co-activator (Goulev et al., 2008; Wu et al., 2008; Zhang et al., 2008a). Given this, and the fact that we and others have identified roles for the Hippo pathway in the *D. melanogaster* CNS (Gailite et al., 2015; Poon et al., 2016; Reddy et al., 2010; Ding et al., 2016), we investigated whether *Sd* operates together with *Yki* to maintain medulla neuron fate. Consistent with prior studies, *Yki* was strongly expressed in the neuroepithelium and low or absent in medulla neurons of the optic lobe (Figures S4A–S4B''') (Gailite et al., 2015; Poon et al., 2016; Reddy et al., 2010). To explore a potential role for *Yki* in medulla neurons, we expressed a hyperactive *Yki* transgene (*Yki*^{S168A}), because *Yki* overexpression phenocopies *Sd-GA* expression in epithelial tissues (Zhang et al., 2008a). Expression of *Yki*^{S168A} using the actin-Gal4 flip-out technique induced overproliferation of the neuroepithelium (Figures S4C–S4C' and S4E–S4E'), as reported earlier (Reddy et al., 2010), but did not induce dedifferentiation of medulla neurons (Figures S4D–S4D' and S4F–S4F'). Finally, co-expression of a different hyperactive *Yki* allele (*Yki*^{3SA}) together with *Sd* in me-

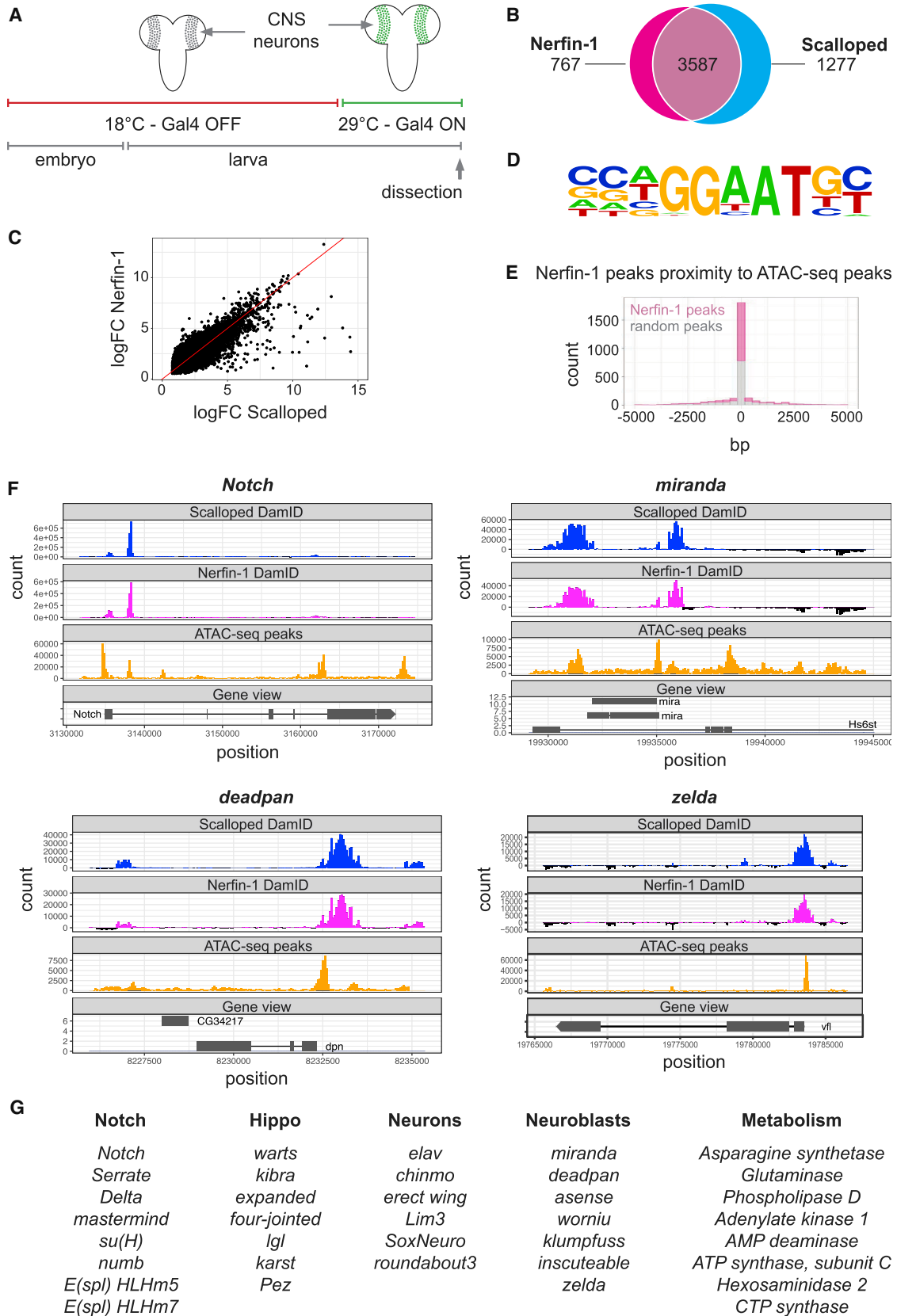
dulla neurons, using the *GMR31H08-Gal4* driver (Li et al., 2014) (active mostly in post-mitotic neurons [Figures S4G–S4H']), also failed to induce dedifferentiation of medulla neurons (Figures S4I–S4J'). Therefore, we conclude that *Sd* regulates medulla neuron fate independent of *Yki*.

Scalloped and Nerfin-1 Occupy a Largely Overlapping Set of Genes in Medulla Neurons

To explore how *Sd* and *Nerfin-1* maintain medulla neuron fate at the molecular level, we set out to identify potential target genes, using the newly developed method of *in vivo* Targeted DamID (Southall et al., 2013). This approach is extremely powerful because it allows transcription factor genome-binding profiles to be identified in precise cell types at specific stages of development (using the heterologous UAS-Gal4 expression system) and alleviates the problematic issues of toxicity and spurious DNA methylation, which can limit the utility of DamID (Southall et al., 2013; van Steensel et al., 2001). We generated transgenic *D. melanogaster* strains expressing transgenes encoding for Dam methylase fused to either *Sd* or *Nerfin-1*. These Dam fusion proteins or a control Dam only fusion protein were expressed for 24 hr from the mid-L3 larval stage, specifically in the neurons of the larval CNS (Figure 5A), using *GMR31H08-Gal4* (Figures S4H–S4H'). This developmental time window was chosen as it aligns with the period when most medulla neurons are generated. Third-instar larval CNS lobes were dissected, methylated DNA was isolated, and next-generation sequencing was performed. Data were analyzed using a custom bioinformatics pipeline (described briefly in STAR Methods and in detail in J.S., J.H.A.V., F.F., L.Y.C., K.F.H., A.T.P., unpublished data) to identify regions of the genome that were preferentially methylated by the Dam-transcription factor fusion proteins compared to Dam alone, and thus detect genomic loci occupied by *Sd* and *Nerfin-1*.

Our bioinformatics analysis of Targeted DamID data identified significant enrichment of 4,864 genes in *Sd* DamID experiments and 4,354 genes in *Nerfin-1* DamID experiments. Strikingly, the majority of target genes of each transcription factor were overlapping, as shown in the Venn diagram (Figure 5B). To further analyze *Sd* and *Nerfin-1* genome binding, we performed a correlation analysis on the relative occupancy of *Sd* and *Nerfin-1* at the 3,587 common target genes. As indicated by a Pearson score of 0.84, the relative genomic occupancy of *Sd* and *Nerfin-1* was strongly correlated (Figure 5C). To identify DNA motifs enriched in the genomic regions bound by *Sd* and *Nerfin-1*, we performed Homer analysis on our DamID datasets. A motif bound by the mammalian *Sd* ortholog TEAD4 (Figure 5D) was the most significantly enriched motif in the *Sd* DamID dataset ($p = 1.0E-12$) and the second most significantly enriched motif in the *Nerfin-1* DamID dataset ($p = 1.0E-15$) (Figures S5A and

brain (J and J', L and L', and N and N') are boxed and magnified in (K) and (K'), (M) and (M'), and (O) and (O'), respectively. EdU⁺ (yellow)/*Mira*⁺ cells (red) are only present in deep sections of *nerfin-1*¹⁵⁹ and *Sd-GA* clones (arrow heads). Scale bars: 50 μ m in (G)–(I'), (J) and (J'), (L) and (L'), and (N) and (N'), and 20 μ m elsewhere. (P) Schematic diagram depicting the EdU pulse-chase experiment. During the 4-hr EdU pulse, EdU (yellow) was incorporated by *Mira*⁺ neuroblasts (red) located in the superficial layer of the CNS. During the 24-hr EdU-free chase, EdU⁺ neurons (produced by EdU⁺ neuroblasts) were displaced into the deep layers of the brain. EdU⁺/*Mira*⁺ cells were never found in control clones in deep CNS sections. In contrast, dedifferentiation of medulla neurons to neuroblasts resulted in the presence of EdU⁺/*Mira*⁺ cells in *nerfin-1*¹⁵⁹ and *Sd-GA* clones found in deep CNS sections. See also Figures S3 and S4.



(legend on next page)

S5B). At the individual gene level, the genome-binding profiles of Sd and Nerfin-1 tightly overlapped, as shown for the *Notch*, *Miranda*, *Deadpan*, and *Zelda* genes (Figure 5F). Interestingly, we observed binding of both Sd and Nerfin-1 to their respective gene loci (Figures S5C and S5D). This suggests that they might regulate each other's gene expression, consistent with data in Figure 2. However, our current data do not allow us to discern between transcriptional or post-transcriptional mechanisms of regulation. Collectively, our Targeted DamID analyses suggest that Sd and Nerfin-1 predominantly operate together to regulate transcription of an overlapping set of target genes in CNS lobe neurons.

To determine which Sd/Nerfin-1 bound genes were expressed in medulla neurons, we first performed RNA sequencing (RNA-seq) on Nerfin-1-GFP⁺ neurons that were isolated by fluorescence-activated cell sorting (FACS) dissociated third-instar larval CNS lobes. The gene expression profile of these neurons closely matched that of neurons derived from ventral nerve cord neurons (Berger et al., 2012) (Figure S5E), consistent with a high degree of biological similarity between these cell types. This observed overlap also provided validation of our neuron isolation strategy. As shown in Figure S5F, 52% of Sd/Nerfin-1-bound genes were expressed in medulla neurons, while 48% were silent. This suggests that Sd and Nerfin-1 are associated both with transcriptionally active and silent genes.

Scalloped and Nerfin-1 Occupy Sites of Regulatory Chromatin

To analyze the global regulatory chromatin landscape in medulla CNS neurons we performed assay for transposase-accessible chromatin with high-throughput sequencing (ATAC-seq), which identifies regulatory chromatin that is in an open conformation, allowing it to be bound by proteins such as transcription factors (Buenrostro et al., 2013). Accessible chromatin corresponds to regions of the genome that are associated with active transcription, as well as regions associated with transcriptional repression (Shlyueva et al., 2014). Larval neurons were isolated by FACS-sorting dissociated CNS lobes that were dissected from the Nerfin-1-GFP strain. The ATAC-seq profile of these neurons identified 35,494 regions of open chromatin, with an average

width of 544 bp. A comparison of ATAC-seq and DamID data showed that the vast majority (90%) of both Nerfin-1 and Sd binding sites were within 600 bp of an ATAC-seq peak, which simulations showed is 1.6-fold higher than expected based on chance (Figures 5E and S5G). The observed enrichment of overlapping ATAC-seq and Nerfin-1 DamID peaks was significant, with a p value of 2.9e-77, and independently verifies that our Targeted DamID studies successfully identified bona fide genome binding sites of Sd and Nerfin-1. We performed gene ontology and Kyoto Encyclopedia of Genes and Genomes (KEGG) analysis on putative shared Sd/Nerfin-1 target genes (Figures 5G, S6A, and S6B) as well as on the sets of genes bound by Sd or Nerfin-1 alone (Figures S6C–S6F). Gene ontology analysis revealed that putative Sd/Nerfin-1 target genes were enriched for general and CNS-specific developmental gene ontology categories, consistent with the hypothesis that they directly regulate expression of genes that mediate dedifferentiation (Figure S6A). KEGG analysis revealed enrichment of key developmental pathway such as Notch and Hippo, as well as multiple metabolic pathways (Figures 5G and S6B).

Expression of Putative Scalloped/Nerfin-1 Target Genes Are Altered When Neurons Dedifferentiate

To investigate whether expression of putative Sd/Nerfin-1 target genes, as determined by DamID, is indeed regulated by these transcription factors, we performed two sets of analyses. We identified Sd/Nerfin-1 target genes that were differentially expressed between wild-type neurons and *nerfin-1*¹⁵⁹ mutant neurons (analysis 1), and those that were differentially expressed in neuroblasts and neurons (as defined by Berger et al., 2012 [analysis 2]), given that perturbation of Sd or Nerfin-1 causes dedifferentiation of neurons to a neuroblast-like fate. To execute analysis 1, we compared RNA-seq data derived from Nerfin-1-GFP⁺ neurons (described above) with RNA-seq data from *nerfin-1*¹⁵⁹ mutant third-instar larval CNS clones (Froldi et al., 2015) to identify differentially expressed genes. Finally, we compared these genes to putative Sd/Nerfin-1 target genes that we identified using Targeted DamID. 602 putative Sd/Nerfin-1 target genes were upregulated in *nerfin-1*¹⁵⁹ mutant clones, while 515 genes were downregulated (Figure 6A). KEGG pathway enrichment analysis revealed Notch

Figure 5. Scalloped and Nerfin-1 Occupy a Largely Overlapping Set of Genomic Loci in Medulla Neurons

(A) Schematic representation of Targeted DamID experiments. The heterologous UAS-Gal4 system was used to precisely target expression of the Sd-Dam or Nerfin-1-Dam transgenes to neurons of the larval CNS. Transgene expression was induced in a precise temporal window, using temperature-sensitive Gal80 (Gal80^{ts}), which represses Gal4-mediated transcription.

(B) A Venn diagram indicating the degree of overlap of genomic loci bound by Sd and Nerfin-1. Significantly, the majority of loci were co-occupied by both transcription factors.

(C) A correlation analysis performed on the relative occupancy of Sd and Nerfin-1 at the 3,587 common occupancy sites, as determined by Targeted DamID. As indicated by a Pearson score of 0.84, the relative occupancy of Sd and Nerfin-1 at genomic loci was strongly correlated.

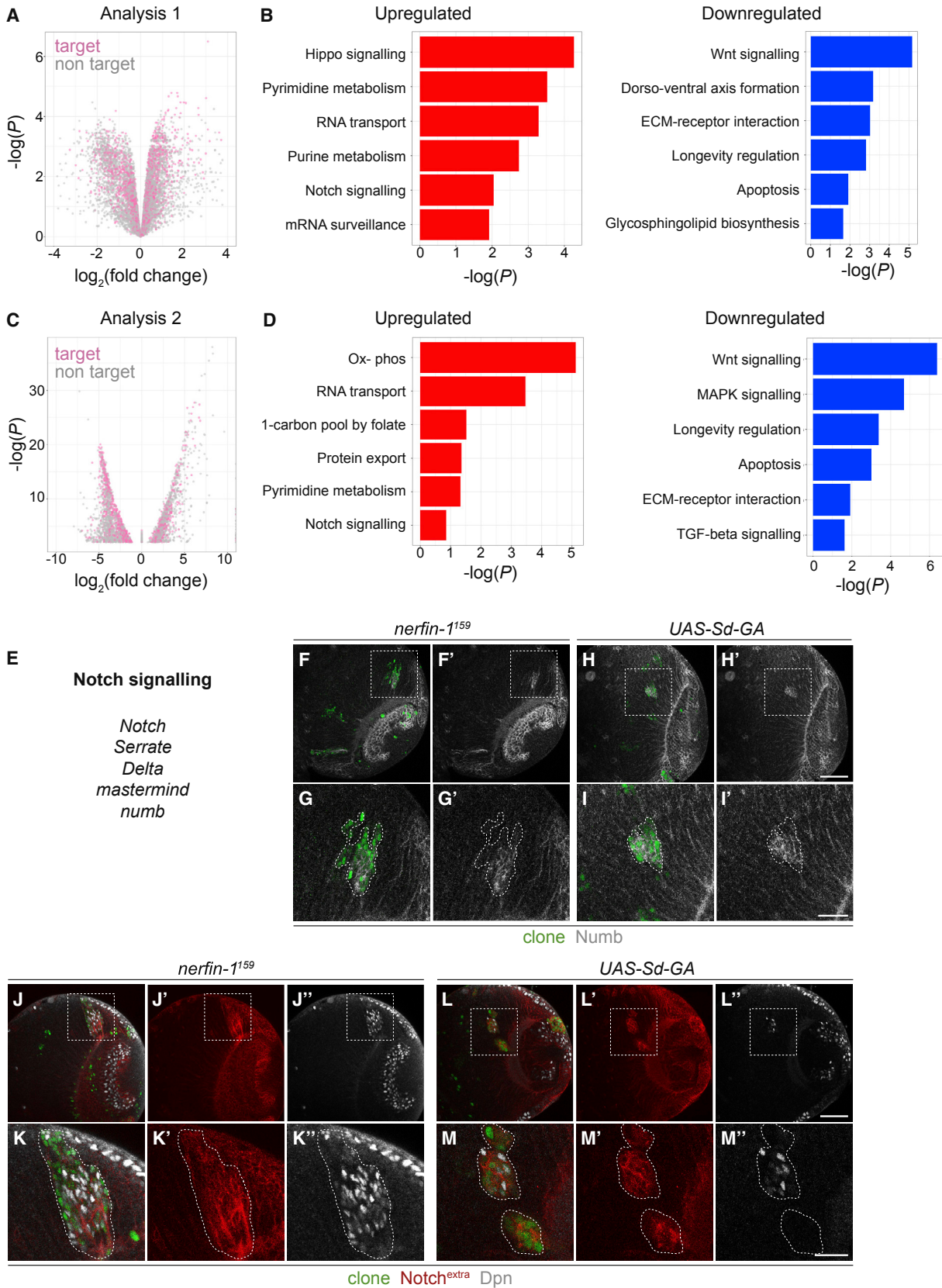
(D) Transcription factor motif analysis revealed a TEAD motif as the most enriched among Scalloped DamID target genes.

(E) Histogram showing the distribution on chromosome arm 2L of Nerfin-1 DamID peaks to ATAC-seq peaks (pink) and also the distance distribution of random peaks to ATAC-seq peaks as background (gray). The bins represent 333 bp each. Compared with the random peaks, DamID peaks were significantly co-localized with ATAC-seq peaks. Five runs of simulations established that the likelihood of this degree of overlap between random peaks and ATAC-seq peaks is highly unlikely (p = 2.9E-77).

(F) Genome-binding profiles of Sd and Nerfin-1, as determined by Targeted DamID, for the *Notch*, *miranda*, *deadpan*, and *zelda* genes. These profiles often closely overlapped and also overlapped with ATAC-seq profiles from third-instar larval CNS lobe neurons.

(G) A sample of genes bound by both Nerfin-1 and Sd. Top scoring pathway and functional categories are shown, together with individual genes from these categories that were bound by both Sd and Nerfin-1.

See also Figures S5 and S6.



(legend on next page)

and Hippo as the top developmental pathways whose expression was elevated, while Wnt pathway genes were among the most downregulated (Figure 6B).

In analysis 2, we compared genes that were differentially expressed in third-instar larval neurons and neuroblasts (Berger et al., 2012) to putative common Sd/Nerfin-1 target genes that we identified using Targeted DamID. 470 candidate Sd/Nerfin-1 target genes were upregulated in neuroblasts versus neurons, while 656 genes were downregulated (Figure 6C). The only developmental pathway that was elevated in KEGG pathway enrichment analysis was the Notch pathway (Figure 6D). Among the most downregulated pathways were Wnt and MAPK pathways (Figure 6D), which have previously been shown to play important roles in neuroepithelial proliferation and the neuroepithelial-to-neuroblast transition (Egger et al., 2007). To validate the above analyses, we assessed a range of common candidate Sd/Nerfin-1 targets whose expression changed in either experiment. Proteins encoded by the neuroblast-specific genes *Mira* and *Asense* as well as the cell cycle regulator *Geminin* were all elevated in *nerfin-1¹⁵⁹* mutant clones and Sd-GA-expressing clones (Figures 3D–D', 3H–H', and S7A–S7D'). Among downregulated genes identified in our analyses were the neuronally expressed genes *Elav*, *Tramtrak*, and *Robo3*. Expression of proteins encoded by these genes was substantially lower when either Nerfin-1 or Sd function was perturbed in medulla neuron clones (Figures S7E–S7J'). Notch pathway genes that were identified as putative Sd/Nerfin-1 target genes, and whose expression was determined as elevated using the above analyses, included the *notch* gene itself, the Notch ligands *delta* and *serrate*, and the transcription factors *Su(H)* and *mastermind* (Figure 6E). Proteins encoded by the Notch pathway genes *Numb*, *Notch*, and *Deadpan* were all elevated when either Nerfin-1 or Sd function were perturbed (Figures 6F–6M'').

The Notch Pathway Mediates Dedifferentiation of Medulla Neurons following Perturbation of Scalloped or Nerfin-1

Next, we pursued a role for the Notch pathway in neuronal fate maintenance downstream of Sd and Nerfin-1 because (1) it was upregulated in both analyses 1 and 2; (2) expression changes in several pathway proteins upon perturbation of Sd and Nerfin-1 could be validated; and (3) it has well-described roles in CNS development. Because forced activation of Sd target genes (via expression of Sd-GA) induced neuronal dedif-

ferentiation, we focused on transcriptional activation of Notch pathway genes as a candidate dedifferentiation mechanism. Initially, we tested whether hyperactivation of the Notch pathway was sufficient to induce neuron-to-neuroblast reversion. We used *GMR31H08-Gal4* to express hyperactive Notch mainly in post-mitotic medulla neurons and observed substantial dedifferentiation in the medulla cortex (Figures 7A–7B', arrowheads). Similarly, substantial dedifferentiation of medulla neurons was induced upon expression of activated Notch protein in MARCM clones (Figures 7C–7E).

Interestingly, a recent report showed that while Notch signaling is not required for generation of neuroblast lineages, its activity is required for dedifferentiation of medulla neurons that ensues follow *nerfin-1* loss (Xu et al., 2017). We confirmed this result by showing that inhibition of Notch pathway activity, via depletion of the Notch ligand Delta, significantly reduced the number of medulla neurons that underwent dedifferentiation in *nerfin-1¹⁵⁹* clones (Figures 7F–7J). Similarly, Delta inhibition suppressed the ability of Sd-GA-expressing medulla neuron clones to undergo neuron-to-neuroblast reversion (Figures 7K–7O). Collectively, these studies indicate that Sd and Nerfin-1 maintain the fate of medulla neurons, at least in part, by repressing activity of the Notch pathway.

DISCUSSION

Scalloped and Nerfin-1 Form a Transcription Factor Pair to Maintain Neuronal Cell Fate

When cells differentiate, they must maintain their fate in a stable manner and repress their ability to adopt alternate cell fates. This is essential for the function of differentiated cells and, when aberrant, can result in pathological consequences. The mechanism by which neuronal cell fate is stably maintained is incompletely understood, with only a handful of factors being linked to this process (Carney et al., 2013; Foldi et al., 2015; Southall et al., 2014). In the present study, we demonstrate that Nerfin-1 maintains the fate of medulla neurons in the optic lobes of the *D. melanogaster* CNS, in partnership with the TEA domain transcription factor Sd. Our data are consistent with the idea that these proteins operate as a transcription factor pair, given that they form a physical complex, and bind to a highly overlapping set of genomic loci. Putative Sd/Nerfin-1 targets were enriched for genes that are functionally associated with the fate of neurons and neuroblasts, cellular metabolism, as well as developmental

Figure 6. Identification of Candidate Scalloped/Nerfin-1 Target Genes by Targeted DamID and RNA-Sequencing

(A) Volcano plot of genes whose expression was higher or lower in wild-type neurons compared to *nerfin-1¹⁵⁹* mutant neurons. Genes that were identified as being occupied by Sd and Nerfin-1 by Targeted DamID are labeled in pink.

(B) KEGG analysis on putative Sd and Nerfin-1 target genes that were upregulated or downregulated in (A).

(C) Volcano plot of genes whose expression was higher or lower in neuroblasts versus neurons. Genes that were identified as being occupied by Sd and Nerfin-1 by Targeted DamID are labeled in pink.

(D) KEGG analysis on putative Sd and Nerfin-1 target genes that were upregulated or downregulated in (C).

(E) Select Notch pathway genes that were identified as candidate Sd/Nerfin-1 target genes.

(F–M'') Third-instar larval CNS lobes containing *nerfin-1¹⁵⁹* mutant MARCM clones (F–G' and J–K'') or Sd-GA-expressing clones (H–I' and L–M'') in the medulla. Clones are marked by GFP (green). The boxed regions in the top panels are magnified in the lower panels, where clones are also outlined. Proteins encoded by putative Sd/Nerfin-1 target genes (*Numb* [grayscale], Notch extracellular domain [red], and *Deadpan* [grayscale]) were elevated in both *nerfin-1¹⁵⁹* clones and Sd-GA-expressing clones. Clones were induced 48 hr AEL and analyzed 72 hr later.

Scale bars: 50 μ m in (F)–(F'), (H)–(H'), (J)–(J''), and (L)–(L''), and 20 μ m elsewhere.

See also Figure S7.

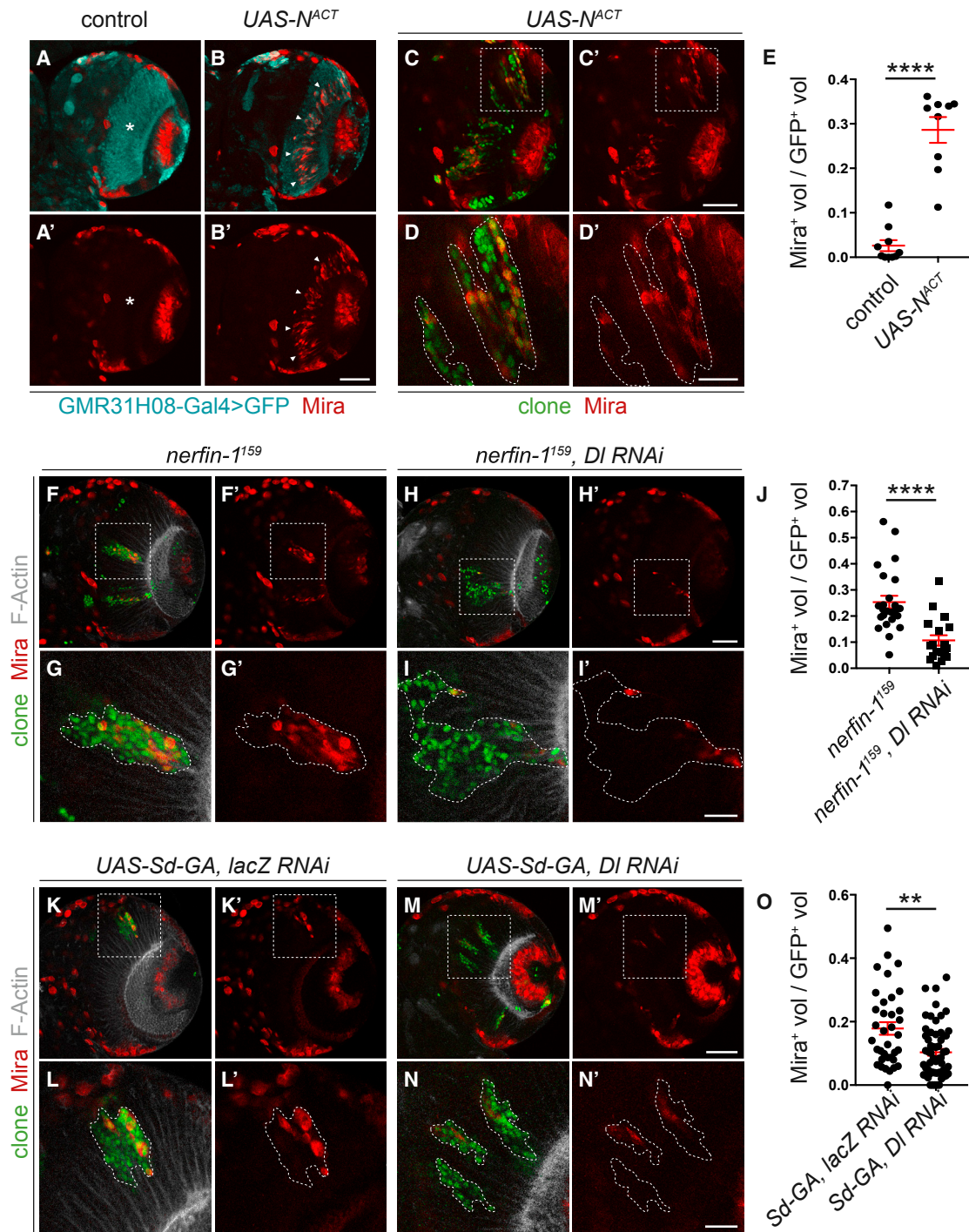


Figure 7. Notch Hyperactivity Is Required for Neuronal Dedifferentiation Triggered by Deregulation of Scalloped or Nerfin-1

(A–B') *GMR31H08-Gal4* was used to drive expression of GFP (A and A') or GFP and activated Notch (*N^{ACT}*) (B and B') in the medulla neurons of the optic lobe. GFP is cyan, and neuroblasts are marked by Mira (red). Ectopic Mira⁺ cells were observed in the medulla layer of the *N^{ACT}*-expressing lobe (arrowheads in B–B') but not in the control lobe (* in A and A'). Embryos were raised at 18°C for 3 days to avoid early lethality and then moved to 29°C until the end of larval development. (C–D') Expression of *N^{ACT}* in medulla MARCM clones (green) resulted in ectopic neuroblast formation (Mira⁺, red) in the medulla neuron layer of the CNS. Clones are outlined, and the boxed regions in (C) and (C') are magnified in (D) and (D'). (E) Quantification of Mira⁺ cells in clones of the genotypes displayed in (C)–(D'); n = 10 and 9, respectively. (F–I') *nerfin-1¹⁵⁹* MARCM clones (F–G') or *nerfin-1¹⁵⁹* MARCM clones expressing *Delta RNAi* (*DI RNAi*; H–I') in the medulla area, stained with Mira (red) and phalloidin, to mark F-Actin (grayscale). The boxed regions in (F), (F'), (H), and (H') are magnified in (G), (G'), (I), and (I'), respectively, where clones are outlined.

(legend continued on next page)

signaling pathways such as Notch and Hippo. Given that forced activation of Sd target genes induced reversion of medulla neurons to neural stem cells (NSCs), we hypothesize that aberrant activation of genes that Sd and Nerfin-1 regulate, is the primary driver of neuronal dedifferentiation in their absence.

The Notch Pathway Is a Key Target of Scalloped and Nerfin-1 in the Context of Neuronal Fate

The Notch pathway was identified as a key target for regulation by Nerfin-1 and Sd, because (1) expression of multiple Notch pathway members was elevated when either Sd or Nerfin-1 function was perturbed; (2) Notch activity was required for dedifferentiation caused by Sd or Nerfin-1 deregulation; and (3) expression of a hyperactive Notch transgene was sufficient to induce dedifferentiation of medulla neurons. Recently, we and others identified a requirement of Nerfin-1 in maintaining the differentiated status of neurons in the ventral nerve cord, central brain, and medulla lineages (Froldi et al., 2015; Xu et al., 2017). The latter study also demonstrated a requirement for Notch hyperactivity in mediating medulla neuron dedifferentiation following *nerfin-1* loss. Here, we extend these studies by showing that Nerfin-1 regulates neuronal maintenance in partnership with Sd. Furthermore, our study demonstrates that these transcription factors promote neuronal fate by regulating the expression of multiple Notch pathway genes.

Neuronal Maintenance in the CNS Is Regulated by Region-Specific Mechanisms

Our data further demonstrate that neuronal cell fate is maintained by distinct factors in different regions of the CNS. In contrast to Nerfin-1, which is required to maintain neuronal differentiation in several neuroblast lineages, Sd is specifically required to maintain the fate of medulla neurons but not neurons derived from ventral nerve cord or central brain neuroblast lineages. The CNS region-specific function of Sd, versus the general requirement for Nerfin-1, is reminiscent of that described for Lola and Prospero, where Lola is required to maintain medulla neuronal fate, but acts redundantly with Prospero in other regions of the CNS (Carney et al., 2013; Southall et al., 2014). Future studies will elucidate the cooperative transcriptional networks that govern neuronal fate maintenance in different regions of the CNS.

Scalloped Controls Medulla Neuron Fate Independent of the Hippo Pathway

Sd function has been best studied in the context of Hippo pathway-dependent tissue growth, where it serves as the key transcription factor of the Yki transcriptional co-activator (Wu et al., 2008; Zhang et al., 2008a; Goulev et al., 2008). Sd has

also been linked to regulation of transcription with other proteins, such as Vestigial (Williams et al., 1993; Halder et al., 1998; Simmonds et al., 1998), Tgi (Guo et al., 2013; Koontz et al., 2013), and in this study, Nerfin-1. Interestingly, the Hippo pathway was among the top signaling pathways identified in KEGG analyses on putative Sd/Nerfin-1 target genes. However, Sd promotes medulla neuronal fate independent of Hippo and Yki, as Yki is not obviously expressed in medulla neurons and cannot induce dedifferentiation. Interestingly, this contrasts with the reported role of Hippo, Yki, and Sd in other neurons. For example, these proteins operate together to control the fate of R8 photoreceptor neurons of the *D. melanogaster* eye. In one class of these light-sensing neurons, Yki and Sd are required to adopt a fate that allows the sensing of blue light, whereas in the other subtype, which senses green light, the Hippo pathway represses Yki and Sd activity (Jukam et al., 2013).

Scalloped and Nerfin-1 Are an Evolutionarily Conserved Transcription Factor Pair

Orthologs of Sd and Nerfin-1 have been functionally linked in both *C. elegans* and vertebrates. In *C. elegans*, EGL-44 and EGL-46 form a physical complex and are both required to specify neuronal cell fate and Q neuroblast differentiation (Feng et al., 2013; Wu et al., 2001). Here, by characterizing both the biochemical interaction of Sd and Nerfin-1 and their role in maintenance of neuronal fate, we show that they cooperate to perform similar functions in flies and worms. The vertebrate orthologs of Sd and Nerfin-1 (TEAD1-4 and INSM1) have also been implicated in various aspects of neural and neuroendocrine development. Murine INSM1 is required for the development of endocrine and neuroendocrine cells of the pancreas, intestine, pituitary, and lung (Feng et al., 2013; Gierl et al., 2006; Jia et al., 2015a, 2015b, Osipovich et al., 2014; Welcker et al., 2013), while in the CNS, it is required for differentiation of neural progenitor cells (Monaghan et al., 2017). Furthermore, zebrafish *insm1a* has been implicated in dedifferentiation in the context of Müller glia regeneration (Ramachandran et al., 2012). Similarly, expression of a TEAD gain-of-function allele caused a marked expansion of the neural progenitor pool in the developing chick neural tube (Cao et al., 2008). Interestingly, preliminary studies suggest that the TEAD/INSM1 pair might also operate together in vertebrates; a motif corresponding to the TEAD binding site was enriched in INSM1 target genes, as determined by INSM1 ChIP-seq performed in murine pancreatic beta cells (Jia et al., 2015a). Our studies of Sd and Nerfin-1 in the *Drosophila* CNS, coupled with the finding that human TEAD1 and INSM1 form a physical complex, further strengthen the idea that these proteins represent an evolutionarily conserved transcription factor pair.

(J) Quantification of Mira⁺ cells in clones of the genotypes displayed in (F)–(G') and (H)–(I'). n = 25 and 18, respectively.

(K–N') Medulla MARCM clones expressing *Sd-GA* and *lacZ RNAi* (K–L'), or clones expressing *Sd-GA* and *DI RNAi* (M–N'), stained for Mira (red) and phalloidin, to mark F-Actin (grayscale). Clones are marked by GFP (green). The boxed regions in (K), (K'), (M), and (M') are magnified in (L), (L'), (N), and (N'), respectively, where clones are outlined.

(O) Quantification of Mira⁺ cells in clones of the genotypes displayed in (K–L') and (M–N'). n = 36 and 60, respectively.

Quantification of Mira⁺ cells (expressed as the ratio between Mira⁺ volume and total GFP⁺ clone volume) in (E), (J), and (O) is represented as mean ± SEM. p values were obtained performing unpaired t test, and Welch correction was applied in case of unequal variances. ****p < 0.0001 and **p < 0.01. Scale bars: 50 μm in (A)–(C'), (F) and (F'), (H) and (H'), (K) and (K'), and (M) and (M'), and 20 μm elsewhere.

STAR★METHODS

Detailed methods are provided in the online version of this paper and include the following:

- [KEY RESOURCES TABLE](#)
- [CONTACT FOR REAGENT AND RESOURCE SHARING](#)
- [EXPERIMENTAL MODEL AND SUBJECT DETAILS](#)
 - Fly strains
 - Clone induction
- [METHOD DETAILS](#)
 - Immunostaining and imaging
 - EdU pulse/chase
 - Clone volume measurements
 - Plasmids
 - Cell culture and transfection
 - Affinity Purification
 - Western blot
 - Targeted DamID
 - DNA Isolation
 - DamID
 - Assay for Transposase-Accessible Chromatin with high throughput sequencing (ATAC-seq)
 - RNA-sequencing
 - Bioinformatics
- [QUANTIFICATION AND STATISTICAL ANALYSIS](#)
- [DATA AND SOFTWARE AVAILABILITY](#)

SUPPLEMENTAL INFORMATION

Supplemental Information includes seven figures and can be found with this article online at <https://doi.org/10.1016/j.celrep.2018.10.038>.

ACKNOWLEDGMENTS

We thank Andrea Brand, Alex Gould, Claude Desplan, Kirsten Guss, Yuh-Nung Jan, Jin Jiang, Alexander Kuzin, Lei Zhang, Michael Lan, Helena Richardson, James Skeath, Tony Southall, Alexey Veraksa, the Vienna *Drosophila* RNAi Center, the Bloomington *Drosophila* Stock Centre, the *Drosophila* Genomics Resource Centre (DGRC), the Australian *Drosophila* Research Support Facility (<http://www.ozdros.com>), and the Developmental Studies Hybridoma Bank (DSHB) for fly stocks, antibodies, and plasmids. We thank Joke van Bommel, Alexey Pindyurin, Owen Marshall, Tony Southall, Mark Dawson, Charles Bell, and Jose Polo for helpful discussions. We thank the Peter Mac Molecular Genomics and Flow Cytometry core facilities and the Centre for Advanced Microscopy and Histology. K.F.H. and A.T.P. are National Health and Medical Research Council (NHMRC) of Australia Senior Research Fellows (1078220 and 116955, respectively). The laboratories of K.F.H. and L.Y.C. were supported by project grants from the NHMRC (1080131 and 1103604). A.T.P. was supported by the Lorenzo and Pamela Galli Charitable Trust and by an NHMRC Program Grant (1054618). The research benefited from support from the Peter MacCallum Cancer Foundation, Victorian State Government Operational Infrastructure Support, and Australian Government NHMRC Independent Research Institute Infrastructure Support.

AUTHOR CONTRIBUTIONS

Conceptualization, J.H.A.V., F.F., J.S., A.T.P., L.Y.C., and K.F.H.; Methodology, J.H.A.V., F.F., J.S., L.Y.C., and K.F.H.; Investigation, J.H.A.V., F.F., J.S., A.T.P., L.Y.C., and K.F.H.; Formal Analysis, J.H.A.V., F.F., and J.S.; Writing – Original Draft, J.H.A.V., F.F., J.S., L.Y.C., and K.F.H.; Supervision, L.Y.C., A.T.P., and K.F.H.; Funding Acquisition, L.Y.C., A.T.P., and K.F.H.

DECLARATION OF INTERESTS

The authors declare no competing interests.

Received: January 31, 2018

Revised: June 14, 2018

Accepted: October 9, 2018

Published: November 6, 2018

REFERENCES

- Berger, C., Harzer, H., Burkard, T.R., Steinmann, J., van der Horst, S., Laursen, A.S., Novatchkova, M., Reichert, H., and Knoblich, J.A. (2012). FACS purification and transcriptome analysis of *Drosophila* neural stem cells reveals a role for Klumpfuss in self-renewal. *Cell Rep.* *2*, 407–418.
- Betschinger, J., Mechtler, K., and Knoblich, J.A. (2006). Asymmetric segregation of the tumor suppressor *brat* regulates self-renewal in *Drosophila* neural stem cells. *Cell* *124*, 1241–1253.
- Bowman, S.K., Rolland, V., Betschinger, J., Kinsey, K.A., Emery, G., and Knoblich, J.A. (2008). The tumor suppressors *Brat* and *Numb* regulate transit-amplifying neuroblast lineages in *Drosophila*. *Dev. Cell* *14*, 535–546.
- Brand, A.H., and Livesey, F.J. (2011). Neural stem cell biology in vertebrates and invertebrates: more alike than different? *Neuron* *70*, 719–729.
- Buenrostro, J.D., Giresi, P.G., Zaba, L.C., Chang, H.Y., and Greenleaf, W.J. (2013). Transposition of native chromatin for fast and sensitive epigenomic profiling of open chromatin, DNA-binding proteins and nucleosome position. *Nat. Methods* *10*, 1213–1218.
- Buszczak, M., Paterno, S., Lighthouse, D., Bachman, J., Planck, J., Owen, S., Skora, A.D., Nystul, T.G., Ohlstein, B., Allen, A., et al. (2007). The carnegie protein trap library: a versatile tool for *Drosophila* developmental studies. *Genetics* *175*, 1505–1531.
- Cao, X., Pfaff, S.L., and Gage, F.H. (2008). YAP regulates neural progenitor cell number via the TEA domain transcription factor. *Genes Dev.* *22*, 3320–3334.
- Carney, T.D., Struck, A.J., and Doe, C.Q. (2013). *midlife crisis* encodes a conserved zinc-finger protein required to maintain neuronal differentiation in *Drosophila*. *Development* *140*, 4155–4164.
- Cebola, I., Rodríguez-Seguí, S.A., Cho, C.H., Bessa, J., Rovira, M., Luengo, M., Chhatriwala, M., Berry, A., Ponsa-Cobas, J., Maestro, M.A., et al. (2015). TEAD and YAP regulate the enhancer network of human embryonic pancreatic progenitors. *Nat. Cell Biol.* *17*, 615–626.
- Choksi, S.P., Southall, T.D., Bossing, T., Edoof, K., de Wit, E., Fischer, B.E., van Steensel, B., Micklem, G., and Brand, A.H. (2006). *Prospero* acts as a binary switch between self-renewal and differentiation in *Drosophila* neural stem cells. *Dev. Cell* *11*, 775–789.
- Ding, R., Weynans, K., Bossing, T., Barros, C.S., and Berger, C. (2016). The Hippo signalling pathway maintains quiescence in *Drosophila* neural stem cells. *Nat. Commun.* *7*, 10510.
- Djiane, A., Krejci, A., Bernard, F., Fexova, S., Millen, K., and Bray, S.J. (2013). Dissecting the mechanisms of Notch induced hyperplasia. *EMBO J.* *32*, 60–71.
- Egger, B., Boone, J.Q., Stevens, N.R., Brand, A.H., and Doe, C.Q. (2007). Regulation of spindle orientation and neural stem cell fate in the *Drosophila* optic lobe. *Neural Dev.* *2*, 1.
- Feng, G., Yi, P., Yang, Y., Chai, Y., Tian, D., Zhu, Z., Liu, J., Zhou, F., Cheng, Z., Wang, X., et al. (2013). Developmental stage-dependent transcriptional regulatory pathways control neuroblast lineage progression. *Development* *140*, 3838–3847.
- Firas, J., Liu, X., Lim, S.M., and Polo, J.M. (2015). Transcription factor-mediated reprogramming: epigenetics and therapeutic potential. *Immunol. Cell Biol.* *93*, 284–289.
- Friedmann-Morvinski, D., and Verma, I.M. (2014). Dedifferentiation and reprogramming: origins of cancer stem cells. *EMBO Rep.* *15*, 244–253.
- Friedmann-Morvinski, D., Bushong, E.A., Ke, E., Soda, Y., Marumoto, T., Singer, O., Ellisman, M.H., and Verma, I.M. (2012). Dedifferentiation of neurons

- and astrocytes by oncogenes can induce gliomas in mice. *Science* 338, 1080–1084.
- Froldi, F., Szuperak, M., Weng, C.F., Shi, W., Papenfuss, A.T., and Cheng, L.Y. (2015). The transcription factor Nerfin-1 prevents reversion of neurons into neural stem cells. *Genes Dev.* 29, 129–143.
- Gailite, I., Aerne, B.L., and Tapon, N. (2015). Differential control of Yorkie activity by LKB1/AMPK and the Hippo/Warts cascade in the central nervous system. *Proc. Natl. Acad. Sci. USA* 112, E5169–E5178.
- Gierl, M.S., Karoulias, N., Wende, H., Strehle, M., and Birchmeier, C. (2006). The zinc-finger factor Insm1 (IA-1) is essential for the development of pancreatic beta cells and intestinal endocrine cells. *Genes Dev.* 20, 2465–2478.
- Goulev, Y., Fauny, J.D., Gonzalez-Marti, B., Flagiello, D., Silber, J., and Zider, A. (2008). SCALLOPED interacts with YORKIE, the nuclear effector of the hippo tumor-suppressor pathway in *Drosophila*. *Curr. Biol.* 18, 435–441.
- Guo, T., Lu, Y., Li, P., Yin, M.X., Lv, D., Zhang, W., Wang, H., Zhou, Z., Ji, H., Zhao, Y., and Zhang, L. (2013). A novel partner of Scalloped regulates Hippo signaling via antagonizing Scalloped-Yorkie activity. *Cell Res.* 23, 1201–1214.
- Gurdon, J.B. (1962). Adult frogs derived from the nuclei of single somatic cells. *Dev. Biol.* 4, 256–273.
- Guss, K.A., Benson, M., Gubitosi, N., Brondell, K., Broadie, K., and Skeath, J.B. (2013). Expression and function of scalloped during *Drosophila* development. *Dev. Dyn.* 242, 874–885.
- Halder, G., Polaczyk, P., Kraus, M.E., Hudson, A., Kim, J., Laughon, A., and Carroll, S. (1998). The Vestigial and Scalloped proteins act together to directly regulate wing-specific gene expression in *Drosophila*. *Genes Dev.* 12, 3900–3909.
- Harzer, H., Berger, C., Conder, R., Schmauss, G., and Knoblich, J.A. (2013). FACS purification of *Drosophila* larval neuroblasts for next-generation sequencing. *Nat. Protoc.* 8, 1088–1099.
- Homem, C.C., and Knoblich, J.A. (2012). *Drosophila* neuroblasts: a model for stem cell biology. *Development* 139, 4297–4310.
- Homem, C.C., Repic, M., and Knoblich, J.A. (2015). Proliferation control in neural stem and progenitor cells. *Nat. Rev. Neurosci.* 16, 647–659.
- Jarman, A.P., Grau, Y., Jan, L.Y., and Jan, Y.N. (1993). atonal is a proneural gene that directs chordotonal organ formation in the *Drosophila* peripheral nervous system. *Cell* 73, 1307–1321.
- Jia, S., Ivanov, A., Blasevic, D., Müller, T., Purfürst, B., Sun, W., Chen, W., Poy, M.N., Rajewsky, N., and Birchmeier, C. (2015a). Insm1 cooperates with Neurod1 and Foxa2 to maintain mature pancreatic β -cell function. *EMBO J.* 34, 1417–1433.
- Jia, S., Wildner, H., and Birchmeier, C. (2015b). Insm1 controls the differentiation of pulmonary neuroendocrine cells by repressing Hes1. *Dev. Biol.* 408, 90–98.
- Jukam, D., Xie, B., Rister, J., Terrell, D., Charlton-Perkins, M., Pistillo, D., Gebelein, B., Desplan, C., and Cook, T. (2013). Opposite feedbacks in the Hippo pathway for growth control and neural fate. *Science* 342, 1238016.
- Kidd, S., Lieber, T., and Young, M.W. (1998). Ligand-induced cleavage and regulation of nuclear entry of Notch in *Drosophila melanogaster* embryos. *Genes Dev.* 12, 3728–3740.
- Knoblich, J.A., Jan, L.Y., and Jan, Y.N. (1997). Asymmetric segregation of the *Drosophila* numb protein during mitosis: facts and speculations. *Cold Spring Harb. Symp. Quant. Biol.* 62, 71–77.
- Koontz, L.M., Liu-Chittenden, Y., Yin, F., Zheng, Y., Yu, J., Huang, B., Chen, Q., Wu, S., and Pan, D. (2013). The Hippo effector Yorkie controls normal tissue growth by antagonizing scalloped-mediated default repression. *Dev. Cell* 25, 388–401.
- Kuzin, A., Brody, T., Moore, A.W., and Odenwald, W.F. (2005). Nerfin-1 is required for early axon guidance decisions in the developing *Drosophila* CNS. *Dev. Biol.* 277, 347–365.
- Kuzin, A., Kundu, M., Brody, T., and Odenwald, W.F. (2007). The *Drosophila* nerfin-1 mRNA requires multiple microRNAs to regulate its spatial and temporal translation dynamics in the developing nervous system. *Dev. Biol.* 310, 35–43.
- Langmead, B., and Salzberg, S.L. (2012). Fast gapped-read alignment with Bowtie 2. *Nat. Methods* 9, 357–359.
- Lee, C.Y., Wilkinson, B.D., Siegrist, S.E., Wharton, R.P., and Doe, C.Q. (2006). Brat is a Miranda cargo protein that promotes neuronal differentiation and inhibits neuroblast self-renewal. *Dev. Cell* 10, 441–449.
- Li, H.H., Kroll, J.R., Lennox, S.M., Ogundeyi, O., Jeter, J., Depasquale, G., and Truman, J.W. (2014). A GAL4 driver resource for developmental and behavioral studies on the larval CNS of *Drosophila*. *Cell Rep.* 8, 897–908.
- Liao, Y., Smyth, G.K., and Shi, W. (2013). The Subread aligner: fast, accurate and scalable read mapping by seed-and-vote. *Nucleic Acids Res.* 41, e108.
- Liao, Y., Smyth, G.K., and Shi, W. (2014). featureCounts: an efficient general purpose program for assigning sequence reads to genomic features. *Bioinformatics* 30, 923–930.
- Liu, W.D., Wang, H.W., Muguira, M., Breslin, M.B., and Lan, M.S. (2006). INSM1 functions as a transcriptional repressor of the neuroD/beta2 gene through the recruitment of cyclin D1 and histone deacetylases. *Biochem. J.* 397, 169–177.
- Marshall, O.J., and Brand, A.H. (2015). damidseq_pipeline: an automated pipeline for processing DamID sequencing datasets. *Bioinformatics* 31, 3371–3373.
- Marshall, O.J., Southall, T.D., Cheetham, S.W., and Brand, A.H. (2016). Cell-type-specific profiling of protein-DNA interactions without cell isolation using targeted DamID with next-generation sequencing. *Nat. Protoc.* 11, 1586–1598.
- Maurange, C., Cheng, L., and Gould, A.P. (2008). Temporal transcription factors and their targets schedule the end of neural proliferation in *Drosophila*. *Cell* 133, 891–902.
- McCarthy, D.J., Chen, Y., and Smyth, G.K. (2012). Differential expression analysis of multifactor RNA-Seq experiments with respect to biological variation. *Nucleic Acids Res.* 40, 4288–4297.
- Monaghan, C.E., Nechiporuk, T., Jeng, S., McWeeney, S.K., Wang, J., Rosenfeld, M.G., and Mandel, G. (2017). REST corepressors RCOR1 and RCOR2 and the repressor INSM1 regulate the proliferation-differentiation balance in the developing brain. *Proc. Natl. Acad. Sci. USA* 114, E406–E415.
- Murawsky, C.M., Brehm, A., Badenhors, P., Lowe, N., Becker, P.B., and Travers, A.A. (2001). Tramtrack69 interacts with the dMi-2 subunit of the *Drosophila* NuRD chromatin remodelling complex. *EMBO Rep.* 2, 1089–1094.
- Neto-Silva, R.M., de Beco, S., and Johnston, L.A. (2010). Evidence for a growth-stabilizing regulatory feedback mechanism between Myc and Yorkie, the *Drosophila* homolog of Yap. *Dev. Cell* 19, 507–520.
- Oh, H., and Irvine, K.D. (2008). In vivo regulation of Yorkie phosphorylation and localization. *Development* 135, 1081–1088.
- Osipovich, A.B., Long, Q., Manduchi, E., Gangula, R., Hipkens, S.B., Schneider, J., Okubo, T., Stoeckert, C.J., Jr., Takada, S., and Magnuson, M.A. (2014). Insm1 promotes endocrine cell differentiation by modulating the expression of a network of genes that includes Neurog3 and Ripply3. *Development* 141, 2939–2949.
- Pindyurin, A.V., Pagie, L., Kozhevnikova, E.N., van Arensbergen, J., and van Steensel, B. (2016). Inducible DamID systems for genomic mapping of chromatin proteins in *Drosophila*. *Nucleic Acids Res.* 44, 5646–5657.
- Poon, C.L., Mitchell, K.A., Kondo, S., Cheng, L.Y., and Harvey, K.F. (2016). The Hippo pathway regulates neuroblasts and brain size in *Drosophila melanogaster*. *Curr. Biol.* 26, 1034–1042.
- Quinn, L.M., Herr, A., McGarry, T.J., and Richardson, H. (2001). The *Drosophila* Geminin homolog: roles for Geminin in limiting DNA replication, in anaphase and in neurogenesis. *Genes Dev.* 15, 2741–2754.
- Ramachandran, R., Zhao, X.F., and Goldman, D. (2012). Insm1a-mediated gene repression is essential for the formation and differentiation of Müller glia-derived progenitors in the injured retina. *Nat. Cell Biol.* 14, 1013–1023.

- Reddy, B.V., Rauskolb, C., and Irvine, K.D. (2010). Influence of fat-hippo and notch signaling on the proliferation and differentiation of *Drosophila* optic neuroepithelia. *Development* *137*, 2397–2408.
- Reiter, F., Wienerroither, S., and Stark, A. (2017). Combinatorial function of transcription factors and cofactors. *Curr. Opin. Genet. Dev.* *43*, 73–81.
- Rhee, D.Y., Cho, D.Y., Zhai, B., Slattery, M., Ma, L., Mintseris, J., Wong, C.Y., White, K.P., Celniker, S.E., Przytycka, T.M., et al. (2014). Transcription factor networks in *Drosophila melanogaster*. *Cell Rep.* *8*, 2031–2043.
- Robinson, M.D., McCarthy, D.J., and Smyth, G.K. (2010). edgeR: a Bioconductor package for differential expression analysis of digital gene expression data. *Bioinformatics* *26*, 139–140.
- Shlyueva, D., Stampfel, G., and Stark, A. (2014). Transcriptional enhancers: from properties to genome-wide predictions. *Nat. Rev. Genet.* *15*, 272–286.
- Simmonds, A.J., Liu, X., Soanes, K.H., Krause, H.M., Irvine, K.D., and Bell, J.B. (1998). Molecular interactions between Vestigial and Scalloped promote wing formation in *Drosophila*. *Genes Dev.* *12*, 3815–3820.
- Southall, T.D., Gold, K.S., Egger, B., Davidson, C.M., Caygill, E.E., Marshall, O.J., and Brand, A.H. (2013). Cell-type-specific profiling of gene expression and chromatin binding without cell isolation: assaying RNA Pol II occupancy in neural stem cells. *Dev. Cell* *26*, 101–112.
- Southall, T.D., Davidson, C.M., Miller, C., Carr, A., and Brand, A.H. (2014). Dedifferentiation of neurons precedes tumor formation in Lola mutants. *Dev. Cell* *28*, 685–696.
- Spitz, F., and Furlong, E.E. (2012). Transcription factors: from enhancer binding to developmental control. *Nat. Rev. Genet.* *13*, 613–626.
- Takahashi, K., Tanabe, K., Ohnuki, M., Narita, M., Ichisaka, T., Tomoda, K., and Yamanaka, S. (2007). Induction of pluripotent stem cells from adult human fibroblasts by defined factors. *Cell* *131*, 861–872.
- Tolhuis, B., Blom, M., and van Lohuizen, M. (2012). Chromosome conformation capture on chip in single *Drosophila melanogaster* tissues. *Methods* *58*, 231–242.
- van Steensel, B., Delrow, J., and Henikoff, S. (2001). Chromatin profiling using targeted DNA adenine methyltransferase. *Nat. Genet.* *27*, 304–308.
- Vogel, M.J., Peric-Hupkes, D., and van Steensel, B. (2007). Detection of in vivo protein-DNA interactions using DamID in mammalian cells. *Nat. Protoc.* *2*, 1467–1478.
- Wang, H., Somers, G.W., Bashirullah, A., Heberlein, U., Yu, F., and Chia, W. (2006). Aurora-A acts as a tumor suppressor and regulates self-renewal of *Drosophila* neuroblasts. *Genes Dev.* *20*, 3453–3463.
- Welcker, J.E., Hernandez-Miranda, L.R., Paul, F.E., Jia, S., Ivanov, A., Selbach, M., and Birchmeier, C. (2013). Insm1 controls development of pituitary endocrine cells and requires a SNAG domain for function and for recruitment of histone-modifying factors. *Development* *140*, 4947–4958.
- Williams, J.A., Paddock, S.W., and Carroll, S.B. (1993). Pattern formation in a secondary field: a hierarchy of regulatory genes subdivides the developing *Drosophila* wing disc into discrete subregions. *Development* *117*, 571–584.
- Wu, J., Duggan, A., and Chalfie, M. (2001). Inhibition of touch cell fate by egl-44 and egl-46 in *C. elegans*. *Genes Dev.* *15*, 789–802.
- Wu, S., Liu, Y., Zheng, Y., Dong, J., and Pan, D. (2008). The TEAD/TEF family protein Scalloped mediates transcriptional output of the Hippo growth-regulatory pathway. *Dev. Cell* *14*, 388–398.
- Xu, J., Hao, X., Yin, M.X., Lu, Y., Jin, Y., Xu, J., Ge, L., Wu, W., Ho, M., Yang, Y., et al. (2017). Prevention of medulla neuron dedifferentiation by Nerfin-1 requires inhibition of Notch activity. *Development* *144*, 1510–1517.
- Yang, L., and Veraksa, A. (2017). Single-step affinity purification of erk signaling complexes using the streptavidin-binding peptide (SBP) tag. *Methods Mol. Biol.* *1487*, 113–126.
- Yasugi, T., Umetsu, D., Murakami, S., Sato, M., and Tabata, T. (2008). *Drosophila* optic lobe neuroblasts triggered by a wave of proneural gene expression that is negatively regulated by JAK/STAT. *Development* *135*, 1471–1480.
- Zhang, L., Ren, F., Zhang, Q., Chen, Y., Wang, B., and Jiang, J. (2008a). The TEAD/TEF family of transcription factor Scalloped mediates Hippo signaling in organ size control. *Dev. Cell* *14*, 377–387.
- Zhang, Y., Liu, T., Meyer, C.A., Eeckhoutte, J., Johnson, D.S., Bernstein, B.E., Nussbaum, C., Myers, R.M., Brown, M., Li, W., and Liu, X.S. (2008b). Model-based analysis of ChIP-Seq (MACS). *Genome Biol.* *9*, R137.
- Zhao, B., Ye, X., Yu, J., Li, L., Li, W., Li, S., Yu, J., Lin, J.D., Wang, C.Y., Chinnaiyan, A.M., et al. (2008). TEAD mediates YAP-dependent gene induction and growth control. *Genes Dev.* *22*, 1962–1971.

STAR★METHODS

KEY RESOURCES TABLE

REAGENT or RESOURCE	SOURCE	IDENTIFIER
Antibodies		
Mouse anti-Mira	Maurange et al., 2008	N/A
Chicken anti-GFP	Abcam	Cat# ab13970; RRID: AB_300798
Rat anti-Elav	DSHB	Cat# 7E8A10; RRID: AB_528218
Guinea pig anti-Nerfin-1	Kuzin et al., 2005	N/A
Rat anti-Sd	Guss et al., 2013	N/A
Mouse anti-Notch ^{extra}	DSHB	Cat# C458.2H; RRID: AB_528408
Guinea pig anti-Dpn	J. Skeath	N/A
Rat anti-Dpn	Abcam	Cat# ab195172
Rabbit anti-Numb	Knoblich et al., 1997	N/A
Rat anti-pH3	Abcam	Cat# ab10543; RRID: AB_2295065
Guinea pig anti-Ase	Jarman et al., 1993	N/A
Rabbit anti-Ttk	Murawsky et al., 2001	N/A
Rat anti-Geminin	Quinn et al., 2001	N/A
Mouse anti-Robo3	DSHB	Cat# 14C9.2H; RRID: AB_528454
Rabbit anti-Yki	Oh and Irvine 2008	N/A
Goat anti-chicken 488	ThermoFisher Scientific	Cat# A11039; RRID: AB_142924
Donkey anti-mouse 555	ThermoFisher Scientific	Cat# A31570; RRID: AB_2536180
Goat anti-mouse 568	ThermoFisher Scientific	Cat# A11019; RRID: AB_143162
Goat anti-guinea pig 568	ThermoFisher Scientific	Cat# A11075; RRID: AB_2534119
Goat anti-rat 568	ThermoFisher Scientific	Cat# A-11077; RRID: AB_2534121
Goat anti-rabbit 633	ThermoFisher Scientific	Cat# A21070; RRID: AB_2535731
Goat anti-guinea pig 647	ThermoFisher Scientific	Cat# A21450; RRID: AB_141882
Goat anti-mouse 647	ThermoFisher Scientific	Cat# A-21235; RRID: AB_2535804
Goat anti-rat 647	ThermoFisher Scientific	Cat# A-21247; RRID: AB_141778
Mouse anti-SBP epitope tag	Santa Cruz Biotechnology	Cat# sc-101595; RRID: AB_1128239
Rabbit anti-HA epitope tag	Sigma-Aldrich	Cat# H6908; RRID: AB_260070
Mouse anti-Myc epitope tag	Santa Cruz Biotechnology	Cat# sc-40; RRID: AB_627268
Mouse anti-Tubulin	Sigma-Aldrich	Cat# T5168 RRID: AB_477579
Rabbit anti-GFP	Abcam	Cat# ab290; RRID: AB_303395
Peroxidase-conjugated AffiniPure Goat Anti-Mouse IgG (H+L)	Jackson ImmunoResearch	Cat# 115-035-003; RRID: AB_10015289
Peroxidase-conjugated AffiniPure Goat Anti-Rabbit IgG (H+L)	Jackson ImmunoResearch	Cat# 111-035-003; RRID: AB_2313567
Goat ANTI-Guinea pig IgG peroxidase conjugate	Sigma	Cat# A7289; RRID: AB_258337
Chemicals, Peptides, and Recombinant Proteins		
Alexa Fluor 633 Phalloidin	ThermoFisher Scientific	Cat# A22284
Streptavidin Plus UltraLink Resin	Pierce	Cat# 53116
HA EZview beads	Sigma	Cat# E6779; RRID: AB_10109562
GFP-Trap beads	ChromoTek	Cat# gta-20; RRID: AB_2631357
Proteinase K	Sigma	Cat# 3115887001
RNaseA	QIAGEN	Cat# 19101
Phase Lock Gel light	5prime	Cat# 2302800
DpnI	NEB	Cat# R0176L
DpnII	NEB	Cat# R0543L
T4 DNA ligase	Sigma	Cat# 10799009001
Advantage I cDNA polymerase mix	Clontech	Cat# 639105

(Continued on next page)

Continued

REAGENT or RESOURCE	SOURCE	IDENTIFIER
Critical Commercial Assays		
Click-iT EdU Alexa Fluor 555 Imaging Kit	Thermo Fisher Scientific	Cat# C10338
Nextera DNA Library Prep Kit	Illumina	Cat# FC-121-1030
MinElute PCR Purification Kit	QIAGEN	Cat# 28004
KAPA Taq EXtra HotStart ReadyMix	Sigma	Cat# KK3604
Deposited Data		
DamID	GSE120731	N/A
ATAC-seq	GSE120731	N/A
RNA-seq	GSE120731	N/A
Experimental Models: Cell Lines		
Human: 293T cells	ATCC	Cat# CRL-3216
<i>D. melanogaster</i> : Stable cell line S2 expressing Scalloped-SBP	This study	N/A
<i>D. melanogaster</i> : Stable cell line S2 expressing Yorkie[S168A]-SBP	This study	N/A
<i>D. melanogaster</i> : Stable cell line S2 carrying empty pMK33-SBP-C vector	This study	N/A
Experimental Models: Organisms/Strains		
<i>w</i> , <i>tub-Gal4</i> , <i>UAS-nlsGFP::6xmyc::NLS</i> , <i>hs-flp</i> ; <i>FRT80B</i> , <i>tubP-Gal80/TM6B</i>	Maurange et al., 2008	N/A
<i>w</i> , <i>tub-Gal4</i> , <i>UAS-nlsGFP::6xmyc::NLS</i> , <i>hs-flp</i> ; <i>FRT2A</i> , <i>tubP-Gal80LL9/TM6B</i>	Maurange et al., 2008	N/A
<i>Df(3L)nerfin-1¹⁵⁹/TM6B</i>	Kuzin et al., 2005	N/A
<i>UAS-Sd-GA/TM6B</i>	Zhang et al., 2008a	N/A
<i>w</i> ; <i>FRT80B</i>	N/A	N/A
<i>yw</i> , <i>hs-flp</i> ; <i>act5 > CD2 > Gal4</i> , <i>UAS-GFP/TM6B</i>	This study	N/A
<i>yw</i> , <i>hs-flp</i> ; <i>act>>Gal4</i> , <i>UAS-RFP/CyO</i> ; <i>UAS-Dcr2/TM6B</i>	This study	N/A
<i>hsflp</i> , <i>act > CD2 > Gal4</i> ; <i>UAS-Dcr2</i> , <i>UAS-GFP</i>	(Xu et al., 2017)	N/A
<i>w¹¹¹⁸</i>	Bloomington Stock Centre	BL3605
<i>sd^{CA07575} (Sd-GFP)</i>	Bloomington Stock Centre	BL50827
<i>nerfin-1.GFP-NLS.SV-40 (Nerfin-1-GFP)</i>	Kuzin et al., 2005	N/A
<i>UAS-sd RNAi</i>	VDRG	KK 101497
<i>UAS-nerfin-1 RNAi</i>	VDRG	KK 101631
<i>UAS-sd</i>	N/A	N/A
<i>UAS-yki^{S168A}</i>	Bloomington Stock Centre	BL28836
<i>UAS-yki^{3SA}</i>	Bloomington Stock Centre	BL28817
<i>UAS-N^{ACT}</i>	Kidd et al., 1998	N/A
<i>UAS-DI RNAi</i>	Bloomington Stock Centre	BL36784
<i>UAS-lacZ RNAi</i>	VDRG	GD 51446
<i>w</i> ; <i>GMR31H08-Gal4</i>	Bloomington Stock Centre	BL49693
<i>w</i> ; <i>tubGal80^{TS}</i> ; <i>GMR31H08-Gal4</i> , <i>UAS-GFP/TM6B</i>	This study	N/A
<i>w</i> ; <i>p[UAST-LT3-Dam-Sd] attP2/TM6B</i>	This study	N/A
<i>w</i> ; <i>p[UAST-LT3-Dam-Nerfin-1] attP2/ TM6B</i>	This study	N/A
<i>w</i> ; <i>p[UAST-LT3-Dam] attP2</i>	This study	N/A
Oligonucleotides		
CTAP_Yki_fwd: ACTGGCTCGAGCAAAATGTGCGCGTGTC	This study	N/A
CTAP_Yki_rev: ACTAGTGGATCCATTAATTTTATACCATTCCAAATCG	This study	N/A
CTAP_Sd_fwd: ACTGGCTCGAGCAAA ATG AAA AAC ATC ACC AGC	This study	N/A
CTAP_Sd_rev: ACTAGTGGATCCTTCCTTAATTAGACGGTATATGTG	This study	N/A
Sd Dam fwd: GCG GCC GCT TAT GAA AAA CAT CAC CAG CTC G	This study	N/A
Sd Dam rev: TCTAGACTATTCCTTAATTAGACGGTATATGTGATG	This study	N/A

(Continued on next page)

Continued

REAGENT or RESOURCE	SOURCE	IDENTIFIER
Nerfin_NotI_fwd: gaa g cgg ccg ctt atgg cccagataca gacac	This study	N/A
Nerfin_XbaI_rev: CGC TCTAGA CTAGTGGGCCATGGTTG	This study	N/A
AdRt: CTAATACGACTCACTATAGGGCAGCG TGGTCGCGGCC GAGGA	Vogel et al., 2007	N/A
AdRb: TCCTCGGCCG	Vogel et al., 2007	N/A
AdR_PCR: GGTCGCGGCCGAGGATC	Vogel et al., 2007	N/A
Recombinant DNA		
pMK33-SBP-C	Yang and Veraksa, 2017	N/A
pMK33-SBP-C Yki S168A	This study	N/A
pMK33-SBP-C Sd	This study	N/A
pUASt-Nerfin-FLAG-HA	<i>Drosophila</i> Genomics Resource Centre	UFO01408
pRK5-MycTEAD1	Zhao et al., 2008	N/A
pcDNA HA-INSM	Liu et al., 2006	N/A
pUASt-HA-Sd	Jin Jiang	N/A
pUASt-LT3-Dam	Southall et al., 2013	N/A
pUASt-LT3-Dam Nerfin-1	This study	N/A
pUASt-LT3-Dam Sd	This study	N/A
Software and Algorithms		
GraphPad Prism	GraphPad Software	https://www.graphpad.com/scientific-software/prism/ ; RRID: SCR_002798
Volocity	Improvision	RRID: SCR_002668
Imaris	Bitplane	http://www.bitplane.com/ ; RRID: SCR_007370

CONTACT FOR REAGENT AND RESOURCE SHARING

Further information and requests for resources and reagents should be directed to and will be fulfilled by the Lead Contact, Kieran Harvey (kieran.harvey@petermac.org).

EXPERIMENTAL MODEL AND SUBJECT DETAILS

Drosophila melanogaster stocks were maintained on standard medium at room temperature (22°C) and experimental crosses were carried out at 18°C, 25°C, or 29°C.

Fly strains

w, *tub-Gal4*, *UAS-nlsGFP::6xmyc::NLS*, *hs-flp*; *FRT80B*, *tubP-Gal80/TM6B*
w, *tub-Gal4*, *UAS-nlsGFP::6xmyc::NLS*, *hs-flp*; *FRT2A*, *tubP-Gal80LL9/TM6B*
Df(3L)nerfin-1¹⁵⁹/TM6B (Kuzin et al., 2005)
P[nerfin-1.GFP-NLS.SV-40] iA (Nerfin-1-GFP, Kuzin et al., 2005).
UAS-Sd-GA/TM6B (Zhang et al., 2008a)
w; *FRT80B*
yw, *hs-flp*; *act5 > CD2 > Gal4*, *UAS-GFP/TM6B*
yw, *hs-flp*; *act >> Gal4*, *UAS-RFP/CyO*; *UAS-Dcr2/TM6B*
hsflp, *act > CD2 > Gal4*; *UAS-Dcr2*, *UAS-GFP* (Xu et al., 2017)
w¹¹¹⁸
sd^{CA07575} (Sd-GFP, #50827 Bloomington Stock Centre)
w; *UAS-nerfin-1*; *UAS-nerfin-1* (A. Kuzin)
UAS-sd RNAi (#KK 101497, VDRC)
UAS-nerfin-1 RNAi (#KK 101631, VDRC)
UAS-sd

UAS-yki^{S168A} (#28836 Bloomington Stock Centre)
UAS-yki^{3SA} (#28817 Bloomington Stock Centre)
UAS-N^{ACT} (Kidd et al., 1998)
UAS-DI RNAi (#36784, Bloomington Stock Centre)
UAS-lacZ RNAi (#GD51446, VDRC)
w; *GMR31H08-Gal4* (#49693 Bloomington Stock Centre)
w; *tubGal80^{TS}*; *GMR31H08-Gal4*, *UAS-GFP/TM6B*

The following transgenic lines for targeted DamID were generated by the Centre for Cellular and Molecular Platforms, National Centre for Biological Sciences, Bangalore, India:

w; *p[pUAST-LT3-Dam-Sd] attP2/TM6B*
w; *p[pUAST-LT3-Dam-Nerfin-1] attP2/ TM6B*
w; *p[pUAST-LT3-Dam] attP2*

Clone induction

All MARCM clones were generated by heat-shocking larvae 48 hr after egg laying (AEL) at 37°C for 20' and dissected 72 hr later, unless otherwise stated. Larvae were transferred and reared at 29°C after heat shock. For the time course analyses in [Figures 4 and S3](#), clones were induced at 96 hr AEL and dissected 16 hr or 24 hr later, or were induced at 72 hr AEL and dissected 48 hr later. Flip-out clones were induced by heat-shocking larvae at 48 hr AEL for 15', and were dissected 72 hr later. *Sd-GA*-expressing flip-out clones were induced at 72 hr AEL to avoid the formation of large neuroepithelial clones.

METHOD DETAILS

Immunostaining and imaging

Larval tissues were fixed in 4% formaldehyde for 20' and immunostained according to standard protocols. Primary antibodies used were: mouse anti-Mira (1:50; [Maurange et al., 2008](#)), chick anti-GFP (1:2000; ab13970, Abcam), rat anti-Elav (1:100; 7E8A10, Developmental Studies Hybridoma Bank), guinea pig anti-Nerfin-1 (1:5000; A. Kuzin), rat anti-Sd (1:10; [Guss et al., 2013](#)), mouse anti-Notch^{extra} (1:50; C458.2H, Developmental Studies Hybridoma Bank), guinea pig anti-Dpn (1:1000; James Skeath), rat anti-Dpn (1:100; ab195172, Abcam), rabbit anti-Numb (1:1000; [Knoblich et al., 1997](#)), rat anti-pH3 (1:800, ab10543, Abcam), guinea pig anti-Ase (1:2000; [Jarman et al., 1993](#)), rabbit anti-Ttk (1:100; [Murawsky et al., 2001](#)), rat anti-Geminin (1:100; [Quinn et al., 2001](#)), mouse anti-Robo3 (1:50, 14C9, Developmental Studies Hybridoma Bank) and rabbit anti-Yki (1:100; [Oh and Irvine, 2008](#)). Secondary goat or donkey antibodies conjugated to Alexa488, Alexa555, Alexa568 and Alexa633 (Molecular Probes, ThermoFisher Scientific) were used at 1:500 and Alexa Fluor 633 Phalloidin (A22284, ThermoFisher Scientific) at 1:200. Images were collected on a Leica SP5 or on a Zeiss Elyra confocal microscope, and all images shown are single sections.

EdU pulse/chase

Control, *nerfin-1¹⁵⁹* or *UAS-Sd-GA* MARCM clones were induced 48 hr AEL. 48 hr after clone induction, larvae were fed with 100 µg/mL EdU for 4 hr. They were then transferred to standard medium for a 24 hr EdU-free chase. Larvae were dissected and processed for antibody staining, and incorporated EdU was detected by Click-iT fluorescent dye azide reaction according to manufacturer instructions.

Clone volume measurements

GFP⁺ and Mira⁺ volume of medulla clones originating from either one or two neuroblasts were measured using fluorescence intensity from three-dimensional reconstructions of 1.5-µm spaced confocal Z stacks with Volocity software (Improvision) or Imaris (Bitplane). The rate of dedifferentiation was represented as the volume of Mira⁺ cells compared to the total GFP⁺ volume of a given clone. In all graphs, error bars represent the standard error of the mean (SEM) and *p* values are calculated by performing two-tailed, unpaired Student's *t* test. The Welch's correction was applied in case of unequal variances. A non-parametric test (Mann-Whitney test) was used when data showed significant deviation from a normal distribution.

Plasmids

The constructs encoding Sd and Yki^{S168A} fused to Streptavidin Binding Protein (SBP) tag were cloned by PCR amplification using

5'-ACTGGCTCGAGCAAAATGTGCGCGTGC-3' and
 5'-ACTAGTGGATCCATTAATTTTATACCATCCAAATCG-3' (Yki)
 5'- ACTGGCTCGAGCAAA ATG AAA AAC ATC ACC AGC -3'
 5' - ACTAGTGGATCCTTCCTTAATTAGACGGTATATGTG -3' (Sd)

XhoI, SpeI digested Yki PCR product was ligated in XhoI, SpeI digested pMK33-SBP-C and SpeI digested Sd PCR product was ligated in EcoRV, SpeI digested pMK33-SBP-C (Yang and Veraksa, 2017). The pUAS-Nerfin-FLAG-HA UFO construct was from the *Drosophila* Genomics Resource Centre. pRK5-MycTEAD1 (Zhao et al., 2008) was from Addgene. pcDNA HA-INSM (Liu et al., 2006) was from Michael Lan. The Targeted DamID constructs encoding Sd and Nerfin-1 fused to Dam methylase were cloned by PCR amplification using

5'- GCG GCC GCT TAT GAA AAA CAT CAC CAG CTC G -3' and
 5'-TCTAGACTATTCCTTAATTAGACGGTATATGTGATG-3' (Sd), using pUAS-HA-Sd (kind gift from Jin Jiang) as a template and;
 5'- gaa g cgg ccg ctt atgg cccagataca gacac - 3' and
 5'- CGC TCTAGA CTAGTGGCCATGGTTG -3' (Nerfin-1), using pUAS-Nerfin-FLAG-HA as a template. NotI, XbaI digested PCR products were ligated in NotI, XbaI digested pUAS-LT3-Dam (Andrea Brand). All newly cloned constructs were verified by sequencing.

Cell culture and transfection

S2 cells were maintained in Schneider's medium (GIBCO) supplemented with 10% FBS (Sigma-Aldrich) and 1% penicillin/streptomycin (GIBCO). For stable transfection, 3 million cells were seeded and transfected with 1ug pMK33-based plasmid DNA using Effectene (QIAGEN). After 48 hr, stably transfected cells were selected using 300ug/ml hygromycin (Invitrogen 10687-010). Cells were selected for ~1 month, after which control untransfected cells had died, and subsequently kept under continuous selection. HEK293T cells were maintained in DMEM medium (GIBCO) supplemented with 10% FBS and 1% penicillin/streptomycin. HEK293T cells were transfected in 10cm dishes using PEI.

Affinity Purification

Streptavidin Binding Protein tagged proteins were purified according to the protocol described in Yang and Veraksa (2017), with minor modifications. Cells were induced with 75mM CuSO₄ overnight, washed in ice-cold PBS twice and lysed in Default Lysis Buffer (DLB) containing 50 mM Tris pH 7.5, 5% glycerol, 0.2% IGEPAL, 1.5 mM MgCl₂, 125 mM NaCl, 25 mM NaF, 1 mM Na₃VO₄, 1 mM DTT and Complete protease inhibitors (04693 124 001, Roche). Lysis was allowed to proceed for 20', after which lysates were cleared by centrifugation. At this point, an input sample was taken for western analysis. The rest of the lysate was incubated with Streptavidin Plus UltraLink Resin (53116, Pierce) for 2 hr at 4°C. Beads were washed with lysis buffer 4x. For western blot analysis, bound proteins were denatured by addition of 1 bed volume of 2x LDS buffer (NP0007, Life Technologies) and incubation at 70°C for 5'. Supernatant was carefully removed and loaded on SDS-PAGE gels. Immuno-precipitation of HA-tagged INSM1A was performed according to the same protocol except that DTT was omitted from DLB, and HA EZview beads (E6779 Sigma) blocked with 2% BSA in DLB were used. Immuno-precipitation of Sd-GFP was performed according to GFP-Trap manufacturer's instructions with the following modifications. Briefly, 150 larval stage L3 brains from *w¹¹¹⁸* and *Sd-GFP* flies were dissected and lysed in 100ul RIPA buffer (150mM NaCl, 1% Triton X-100, 0.5% Na Deoxycholate, 0.1% SDS, 50mM Tris pH 7.4, 0.5mM EDTA, 2.5mM MgCl₂, 1 μL RQ1 RNase-free DNase (Promega) and Complete protease inhibitors). Lysates were incubated on ice 30' with extensive pipetting every 10', before centrifugation 20000xg 10' at 4°C. Supernatant was diluted in 150ul dilution buffer (150mM NaCl, 0.5mM EDTA, 10mM Tris pH7.5, Complete protease inhibitors), and an input sample was taken for western analysis. The diluted lysate was then added to 10 μL GFP-Trap beads (gta-20, chromotek beads prewashed 3x in dilution buffer). Immunoprecipitation was allowed to proceed 1hr15' at 4°C. Beads were washed 3x in dilution buffer. Finally, bound proteins were denatured by addition of 25 μL of 2x LDS buffer (NP0007, Life Technologies) and incubation at 95°C for 10'. Supernatant was carefully removed and loaded on SDS-PAGE gels.

Western blot

NuPage 4%–12% BisTris SDS-PAGE gels were purchased from Life Technologies and run at 200V in 1x MOPS buffer supplemented with antioxidant. Proteins were transferred to methanol-activated Immobilon membrane (IPVH00010, Millipore) in transfer buffer (50mM Tris, 192mM Glycine, 20% ethanol) in ice 1.5 hr at 110V. Membranes were blocked in 5% (w/v) powder milk dissolved in Tris buffered Saline with 0.1% Tween (TBS/T) at least 30' at RT. Membranes were incubated with primary antibodies o/n at 4°C in blocking buffer, washed 3x 10' in TBS/T, incubated with HRP-coupled secondary antibodies 45' RT, and washed 3x 10' in TBS/T. Membranes were incubated with ECL Prime (RPN2232, GE Healthcare) and western blot data were detected using a BioRad Chemidoc system. Primary antibodies were specific to SBP epitope tag (mouse sc-101595, Santa Cruz), HA epitope tag (Rabbit H6908, Sigma), Myc epitope tag (Mouse 9E10, sc-40 Santa Cruz) and Tubulin (mouse, T5168, Sigma).

Targeted DamID

D. melanogaster crosses and staging

Crosses producing larvae with the following genotypes were allowed to lay eggs o/n at 25°C:

w; + / *tub-Gal80^{ts}* ; *UAS-LT3-Dam/ GMR31H08-Gal4*
w; + / *tub-Gal80^{ts}* ; *UAS-LT3-Dam-Sd/ GMR31H08-Gal4*
w; + / *tub-Gal80^{ts}* ; *UAS-LT3-Dam-Nerfin-1/ GMR31H08-Gal4*

Eggs were transferred to the non-permissive temperature (18°C) for 4 days. To restrict expression of the TaDa transgenes to a defined period, larvae were transferred to the permissive temperature (29°C) 24 hr before dissection. CNSs from wandering third instar larvae were dissected, their ventral nerve cord removed and collected in PBS on ice. CNSs were transferred to 100 μ L ice-cold TENS buffer containing 100 mM Tris, pH 8.0, 5 mM EDTA, 200 mM NaCl, 0.2% SDS and stored at -20°C until further processing. Per experiment ($n = 2$), approximately 300 CNSs were dissected for each genotype.

DNA Isolation

DNA isolation was based on [Tolhuis et al. \(2012\)](#). 2 μ L Proteinase K (20 mg/ml) solution was added followed by overnight incubation at 56°C. Next, RNA was digested 30 mins at 37°C using 0.5 μ L RNase A (100 mg/ml). DNA was extracted by addition of 100 μ L Tris pH8.0 saturated phenol:chloroform:iso amylalcohol (25:24:1 - Sigma), gentle mixing, and separation using phase lock gel light (5prime, cat. # 2302800), according to manufacturer's instructions. The upper phase was transferred to fresh tubes and precipitated by addition of 1 μ L glycogen (20 mg/ml), 10 μ L 3 M NaAc (pH 5.2), 300 μ L EtOH, storage at -80°C for 30' and centrifugation (30mins 14000 rpm 4°C). DNA pellets were washed with 500 μ L 70% EtOH, air-dried briefly and dissolved in 10-25 μ L Tris 10mM pH8. The DNA was not resuspended by pipetting, to prevent DNA shearing. DNA concentration was measured by nano-drop and adjusted to 50ng/ μ L. Samples were stored at -20°C until further processing.

DamID

Our DamID protocol was based on [Marshall et al. \(2016\)](#), [Southall et al. \(2013\)](#), and [Vogel et al. \(2007\)](#). Briefly, 425ng DNA was digested overnight in 10 μ L reactions containing 1 μ L 10x CutSmart buffer (NEB) and 0.5 μ L DpnI (10 units) at 37°C. As a control, one sample was incubated with mix without DpnI. The next morning, 0.5 μ L DpnI, was added for 1 hr extra incubation, followed by DpnI heat inactivation (20 mins 80°C). Adaptor ligation was performed by addition of 6.2 μ L H₂O, 0.8 μ L 50uM ds adaptor AdR (40pmol), 2.0 μ L 10x ligation buffer and 1.0 μ L T4 DNA ligase (5U/ μ L), or the mix minus ligase as a control. Ligation reactions were incubated 2 hr 16°C and stopped by incubation for 10mins at 65°C. Samples were digested with DpnII addition of 1 μ L NEB DpnII buffer, 0.2 μ L DpnII (50U) and 28.8 μ L MQ followed by incubation at 37°C 2 hr. For the mePCR, 10 μ L 10x cDNA PCR Buffer (Clontech; 639105 Scientifix), 2.5 μ L Primer AdR (50uM), 8 μ L dNTPs (2.5mM each), 2 μ L PCR Advantage enzyme (Clontech) and 52.5 μ L H₂O was added to 25 μ L DpnII digested DNA. The PCR program was as follows:

68°C 10 min
94°C 30 s; 65°C 5 min; 68°C 15 min (1 cycle)
94°C 30 s; 65°C 1min; 68°C 10 min (3 cycles)
94°C 30 s; 65°C 1 min; 68°C 2 min (14 cycles)
68°C 5 mins

3 μ L mePCR product was loaded on agarose gel. If a smear was detected in the experimental sample, but not in the controls lacking DpnI and ligase, the mePCR product was purified using QIAGEN PCR purification kit. Libraries for next generation sequencing were prepared as in [Pindyurin et al. \(2016\)](#) with some modifications. Briefly, 3 μ g of purified mePCR product was sonicated using a Covaris S2 device to generate fragments of 100-500bp, with an average of 300bp. DNA was purified using Agencourt AMPure beads purification (Beckman Coulter, cat. no. A63881). The material was measured using a Bioanalyzer 2100 DNA 1000 chip. Illumina sequencing libraries were prepared using KAPA Hyper prep kit (Kapa Biosystems) and 300ng starting material. Five to seven cycles of PCR were performed. Libraries were quantified on a Bioanalyzer 2100 DNA 1000 chip.

Assay for Transposase-Accessible Chromatin with high throughput sequencing (ATAC-seq)

ATAC-seq was performed in biological triplicate. Approximately 500,000 Nerfin-1-GFP⁺ neurons were isolated from larval L3 stage CNS lobes according to [Berger et al. \(2012\)](#) and [Harzer et al. \(2013\)](#). Briefly, optic lobes were dissected in PBS and dissociated using papain and collagenase I. Neurons were sorted using flow cytometry. Cells were washed with ice cold PBS and lysed in 500 μ L lysis buffer containing 10mM Tris-HCl pH7.4, 10mM NaCl, 3mM MgCl₂ and 0.1% IGEPAL CA-630. Nuclei were pelleted by centrifugation 500 rcf . 10'. Lysis buffer was removed and nuclei were resuspended in tagmentation master mix containing 25 μ L TD buffer, 22.5 μ L H₂O and 2.5 μ L transposase (Nextera kit, FC-121-1030, Illumina). Samples were incubated 30' 37°C. DNA was purified using MinElute columns (28004, QIAGEN) and eluted in 20 μ L. For the PCR, 2.5 μ L of forward and reverse indexing primers (25 μ M) and 25 μ L HotStart KAPA ready mix (2x) was added. The PCR program was as follows:

72°C 5 min
98°C 3 min
98°C 20 s; 65°C 15 s; 72°C 1 min (13 cycles)

Amplified libraries were purified using Minelute column (QIAGEN), eluted in 50 μ L and quantified by Qubit/TapeStation. Size distribution and yield of amplified DNA was checked using the TapeStation 2200 (Agilent Technologies). Fragments between 200-700bp were size-selected using a Pippin Prep instrument (1.5% agarose cassette, Sage Science). Libraries were then pooled and sequenced on a NextSeq500 (Illumina). 36-50 million paired-end 75bp reads were generated per sample.

RNA-sequencing

Nerfin-1-GFP⁺ neurons were isolated from larval L3 stage CNS lobes as described under ATAC-seq, pelleted and resuspended in Trizol. RNA was isolated according to manufacturer's protocol. Samples from sorts executed on different days were pooled into three different samples containing 180-330ng RNA. Libraries prepared according to standard protocols (TruSeq RNA, Illumina).

Bioinformatics

DamID-seq analysis

The DamID samples and controls were sequenced on Illumina instruments (HiSeq and NextSeq) in several batches with different protocols. For each sample, two biological replicates were generated (20-60M reads per replicate). Alignment to the reference (dm6) was performed with Subread Subread (v1.5.1) (Liao et al., 2013) and assigning to GATC targets (hereafter referred to as tags) with FeatureCounts (v1.5.1) (Liao et al., 2014). EdgeR (v3.14.0) (McCarthy et al., 2012; Robinson et al., 2010) was used to establish differentially methylated tags comparing Dam-only controls to Nerfin-1-Dam, and Sd-Dam samples. EdgeR was chosen over existing tools (such as Marshall and Brand, 2015) for its ability to correct for batch effects and integrate biological replicates into the analysis. We used TMM normalization on the data. The analysis resulted in 46k significantly methylated tags for Sd and 33k for Nerfin-1, after multiple hypothesis testing correction. Methylated tags were aggregated into peaks, which correspond to protein-DNA binding events. Target genes were established by selecting the closest transcription start site to each peak. A more detailed description of our DamID analysis method will be published elsewhere. To identify DNA motifs enriched in the genomic regions bound by Scalloped and Nerfin-1, we performed Homer (findMotifsGenome, version 4.10.3) analysis on our DamID datasets. Homer was run on the peak regions identified as DamID targets, specifying the reference genome (dm6) as background.

ATAC-seq analysis

Three replicates of ATAC sequencing data were sequenced on an Illumina Nextseq. The samples had around 48, 67, and 66 million reads and aligned to the reference with Bowtie2 (c.2.2.9) (Langmead and Salzberg, 2012) at 100% mapping rate. Macs (v2.1.0) (Zhang et al., 2008b) was used to analyze each of the samples for peaks, indicating open regions of chromatin. The individual results of 40k, 40k, and 42k peaks were intersected to a consensus set of 35k peaks.

RNA-seq analysis

The RNA sequencing samples were comprised of three replicates produced on Illumina NextSeq (SE, 52-68 million reads/sample). Using Subread, a mapping rate of 92% was detected (counting multi-mapping reads as unmapped). FeatureCounts detected on-target rates of 86%-88%. Gene counts were analyzed with EdgeR; genes that did not reach a minimum of 2 CPM between the replicates were discarded from further analysis. After normalization and dispersion estimation, expressed genes were defined as meeting a conservative threshold of at least 10 replicated RPKM.

QUANTIFICATION AND STATISTICAL ANALYSIS

Statistical analysis was carried out using GraphPad Prism 7. Details of statistical tests performed can be found in figure legends and in Methods Details of STAR Methods. Data was reported as mean \pm SEM. Significance was defined as $p < 0.05$.

DATA AND SOFTWARE AVAILABILITY

The accession number for the DamID, RNA-seq, and ATAC-seq data reported in this paper is GEO: GSE120731.